

UNIVERSIDADE DE LISBOA
FACULDADE DE CIÊNCIAS
DEPARTAMENTO DE BIOLOGIA ANIMAL



Ciências
ULisboa

**Phytoplankton response to nutrient pulses in an upwelling
region: microcosms experiments**

Afonso Miguel Barros Barreto Ferreira

Mestrado em Ecologia Marinha

Dissertação orientada por:
Doutora Ana C. Brito

2016

“Afortunadamente, el contacto con la Naturaleza hace ver continuamente la limitación de nuestros esquemas y lo poco que sabemos.”

Ramón Margalef, Ecología

ACKNOWLEDGEMENTS

Em primeiro lugar, gostaria de agradecer à Doutora Ana C. Brito. Por todo o apoio, por toda a motivação e por toda a paciência que teve durante a orientação da tese. Obrigado também por ser um exemplo como investigadora e por estar sempre disponível para me ajudar.

Não poderia deixar também de destacar e agradecer às seguintes pessoas pelo papel fundamental que tiveram na realização deste trabalho: Carolina Sá, Nelson Silva, Ana Margarida Dias e Carolina Beltrán. Obrigado também pela disponibilidade para tirar dúvidas e pela grande ajuda nesta fase final.

Gostaria ainda de agradecer a todas as pessoas que ajudaram no trabalho de laboratório, seja cá ou no Chile, em especial aos seguintes: Ana Amorim, Paola Reinoso, Randy Finke, Ricardo Calderón, Ricardo Prego, Sylvain Faugeron, Vanda Brotas, Vera Veloso e Wiebe Kooistra.

À Professora Isabel Domingos, pelo encorajamento e por procurar sempre defender os alunos do seu mestrado.

A todos os meus amigos que acompanharam durante este processo. Desde o pessoal da Madeira, aos amigos da licenciatura e mestrado (tanto de Ecologia Marinha como de Ecologia e Gestão Ambiental). Sem vocês, teria sido bem mais complicado manter a minha sanidade mental ao longo deste ano.

Por fim, um obrigado especial à Rita e à minha família, em especial aos meus pais e à Teresa.

The work hereby presented has been submitted to an international journal as follows:

Ferreira, A.M., Sá, C., Silva, N., Beltrán, C., Dias, A.M., Brito, A.C., submitted. Phytoplankton response to nutrient pulses in an upwelling region: microcosms experiments. *Journal of Experimental Marine Biology and Ecology*.

Note that the actual content of the paper and the work present in this dissertation is different.

ABSTRACT

The occurrence of nutrient enrichment in coastal areas can, in severe cases, lead to serious disturbances in marine ecosystems. Much is still to be done to understand how phytoplankton communities respond to natural and anthropogenic enrichment. This knowledge is essential to evaluate the implications on ecosystem functioning. The main goal of this study is to understand the response of phytoplankton communities to pulse nutrient enrichments in a region of intense upwelling conditions, namely the Humboldt Current System. In order to achieve this, a microcosm experiment with natural assemblages was conducted. In this experiment, two different experimental treatments were established to achieve N or P-limitation in the microcosms. The microcosms were enriched at the beginning and at half the duration of the experiment. Laboratory work included the analysis of nutrients, as well as phytoplankton pigments (HPLC) and cell abundances (microscopy). The phytoplankton community structure was also evaluated using chemotaxonomy (HPLC-CHEMTAX). Post-bloom conditions were observed at the beginning of the experiment, characterized by high content of chlorophyll *a* degradation products. A fast response to the initial enrichment was observed in both treatments as biomass increased from day 0 to 1. After the second enrichment pulse, a new biomass increase was observed as cell abundances peaked on Day 4. However, abundances slightly dropped in the remainder of the experiment. Although higher biomass values were found under higher DIN concentrations, the community's composition was similar in both experimental treatments. Centric diatoms, especially *Chaetoceros* sp., dominated samples in both enrichments, suggesting growth advantages. Phytoflagellates and pennate diatoms were also common, while abundances of dinoflagellates, on the other hand, were low. HPLC-CHEMTAX results were not in agreement with the ones obtained from cell counts, possibly due to changes in the cells' pigment content. These studies are relevant for understanding the functioning of phytoplankton communities and its influence on the whole ecosystem dynamics, thus being helpful for environmental quality assessment and management of marine resources.

Keywords: Phytoplankton Assemblage, Microcosm Experiments, Nutrient enrichment, HPLC-CHEMTAX, microscopy, Coastal upwelling system

RESUMO ALARGADO

O enriquecimento em nutrientes de zonas costeiras pode advir de diferentes fontes, podendo causar graves distúrbios nos ecossistemas marinhos. Este enriquecimento em nutrientes pode levar a que ocorra eutrofização, podendo esta ser classificada como antropogénica ou natural, consoante a origem do enriquecimento. Nos casos de origem antropogénica, esta pode ocorrer, por exemplo, devido à escorrência de compostos químicos provenientes de atividades humanas ou devido à deposição atmosférica de gases. Já nos casos em que a origem apresenta um carácter natural, as causas mais comuns são o transporte fluvial de nutrientes, quando não influenciado pelo Homem, ou o afloramento costeiro (*upwelling*). Este último é particularmente importante nos quatro sistemas de afloramento costeiro de fronteira oriental: a Corrente da Califórnia, a Corrente das Canárias, a Corrente de Benguela e a Corrente de Humboldt. Estes sistemas, apesar de ocuparem apenas 2% do oceano, contribuem para mais de 20% do total de peixe capturado a nível global. O Sistema da Corrente de Humboldt, que se estende desde cerca dos 42°S até ao equador e engloba a costa do Equador, Perú e parte da costa do Chile, distingue-se dos restantes pela sua elevada produtividade pesqueira. O enriquecimento em nutrientes proveniente do afloramento costeiro é extremamente importante para as comunidades marinhas locais, principalmente para os produtores primários. O fitoplâncton, como componente basal das teias tróficas marinhas, tem um papel muito importante para o funcionamento do ecossistema. Como tal, qualquer alteração ambiental que afete as comunidades fitoplanctónicas, seja na turbulência da coluna de água ou na disponibilidade de luz ou em nutrientes, poderá ter consequências nos restantes elementos da teia trófica. Deste modo, é de extrema importância compreender-se como as comunidades de fitoplâncton respondem a enriquecimentos em nutrientes, quer estes sejam de origem natural ou antropogénica. Este conhecimento é essencial para se conseguir avaliar os potenciais impactos de alterações ambientais no funcionamento do ecossistema. Uma das melhores ferramentas disponíveis para se avaliar a dinâmica do fitoplâncton e a sua relação com enriquecimentos em nutrientes é a realização de experiências laboratoriais com comunidades naturais.

Deste modo, o principal objetivo deste trabalho é compreender a resposta de uma comunidade de fitoplâncton ao enriquecimento em nutrientes numa região com elevada intensidade de *upwelling*. De forma a atingir este objetivo, foram estabelecidas diversas metas específicas: i) avaliar a resposta a nível da biomassa a eventos de enriquecimento em nutrientes previamente estipulados; ii) estudar a sucessão da comunidade durante e após o enriquecimento; iii) averiguar se a comunidade reage de forma diferente a eventos discretos de enriquecimento em nutrientes com composições distintas; iv) analisar se o uso complementar de uma abordagem quimiotaxonómica (HPLC-CHEMTAX) pode fornecer informações adicionais de elevada relevância.

De forma a cumprir estes objetivos, foi realizada uma experiência com recurso a microcosmos que durou seis dias. A recolha de água para a experiência foi efetuada junto à baía de Algarrobo, na zona central do Chile (30-40°S). Foram estabelecidos dois tratamentos experimentais: o tratamento N-limited (limitado em azoto) e o tratamento P-limited (limitado em fósforo). Nestes tratamentos, o objetivo era submeter a comunidade de fitoplâncton a condições de limitação em azoto ou fosfato, consoante o tratamento, de acordo com o rácio de Redfield (N-limited = N:P < 16:1; P-limited = N:P >16:1). Para tal, os microcosmos foram enriquecidos com uma solução que continha nitrato (NO₃-), fosfato (PO₄³⁻) e ácido silícico (Si[OH]₄). A concentração de nitrato e fosfato adicionada aos microcosmos foi ajustada de acordo com cada tratamento. O conteúdo em nutrientes, nomeadamente em azoto inorgânico dissolvido (DIN) e fosfato, foi analisado ao longo da experiência. A comunidade

fitoplanctónica foi também estudada através de contagens de células por microscopia e da análise dos pigmentos fotossintéticos via cromatografia líquida de alto desempenho (HPLC). Por fim, os resultados provenientes da HPLC foram utilizados para, através do programa de quimiotaxonomia CHEMTAX v1.95, estimar a biomassa relativa dos principais grupos de fitoplâncton existentes nos microcosmos.

Analisando dados ambientais das duas semanas anteriores à experiência para a costa do Chile, os baixos valores da temperatura da superfície da água do mar e a existência de ventos perpendiculares de média intensidade junto à costa apontam para a existência de condições favoráveis à ocorrência de afloramento costeiro. Os valores de clorofila *a* observados ($>1 \text{ mg m}^{-3}$) parecem corroborar esta condição, principalmente nas semanas antes da experiência. A elevada concentração de pigmentos associados à degradação da clorofila *a* encontrada nos microcosmos aponta na mesma direção e sugere que a comunidade de fitoplâncton estudada estava num estado pós-florescência (*bloom*).

A comunidade respondeu de forma rápida ao enriquecimento inicial, aumentando a sua biomassa logo no primeiro dia da experiência. Este aumento foi observado tanto para a clorofila *a* como para a abundância de células em ambos os tratamentos. Devido ao crescimento do fitoplâncton, houve um grande consumo dos nutrientes, principalmente de DIN. Ao segundo e terceiro dia houve um declínio da abundância de fitoplâncton no tratamento N-limited, enquanto tal não se verificou no tratamento P-limited, onde se verificou inclusive um máximo no terceiro dia. Esta diferença pode estar relacionada com a disponibilidade de nutrientes nos microcosmos, i.e., a concentração de DIN no tratamento N-limited pode não ter sido o suficiente para promover o crescimento do fitoplâncton. Relativamente à comunidade fitoplanctónica, o principal grupo a ser beneficiado foi o das diatomáceas, em especial as diatomáceas cêntricas. Na verdade, observou-se um domínio de células de diatomáceas. Este domínio é algo recorrente em sucessões de upwelling e pode ser explicado pelas vantagens que este grupo apresenta no que diz respeito à assimilação de grandes concentrações de nutrientes e pela falta de predadores. O género *Chaetoceros*, em particular, devido ao seu domínio ao nível das abundâncias, mostrou ser uma componente bastante relevante para o funcionamento do ecossistema e a sua dinâmica deve ser tida em conta na gestão dos recursos marinhos desta região. Outro grupo comum nas amostras foi o dos fitoflagelados, principalmente das classes Chrysophyceae e Cryptophyceae. Por outro lado, as contagens de dinoflagelados foram relativamente baixas. Em relação ao segundo enriquecimento, houve um novo aumento das abundâncias de fitoplâncton em ambos os tratamentos. No entanto, após atingirem um máximo no quarto dia da experiência, as abundâncias sofreram um declínio. Tendo em conta que ainda parecia haver concentrações de nutrientes suficientes para o crescimento, especula-se que o crescimento da comunidade poderá ter sido limitado por um micronutriente (e.g. Fe), sendo que já foi reportado limitação em Fe para o sistema de afloramento costeiro de Humboldt. O segundo enriquecimento não pareceu ter tido um impacto significativo na estrutura da comunidade, uma vez que as abundâncias relativas dos principais grupos se mantiveram similares ao que tinha sido observado após o enriquecimento inicial. No geral, concluiu-se que, as comunidades de fitoplâncton estudadas reagiram de forma semelhante a enriquecimentos em nutrientes com composições distintas, embora as abundâncias observadas tenham sido mais elevadas no tratamento P-limited.

No entanto, a análise dos pigmentos fitoplanctónicos, incluindo o software CHEMTAX, revelou resultados contraditórios. Nestes, houve uma queda abrupta dos principais pigmentos fotossintéticos encontrados na amostra, como clorofila *a* ou a fucoxantina, a partir do segundo dia da experiência. Pensa-se que tal poderá ter acontecido devido à ocorrência de fotoaclimação, ou seja, as células terão otimizado a sua absorção de fotões, através da diminuição da concentração de clorofila *a* e de outros pigmentos fotossintéticos, de forma a evitar que a elevada luz incidente levasse a danos irreversíveis nos seus fotossistemas. Embora os microcosmos estivessem protegidos de radiação solar direta, é possível que esta proteção não tenha sido suficiente, levando então à fotoaclimação. Uma

forma de evitar que isto aconteça em estudo futuros seria, por exemplo, aumentar a proteção solar.

Os resultados deste estudo são relevantes para perceber o funcionamento das comunidades de fitoplâncton e os seus efeitos na dinâmica do ecossistema, podendo ser úteis para a avaliação de qualidade ambiental e gestão de recursos em habitats aquáticos. Para além disto, esta informação pode ser também utilizada na gestão de problemas relacionados com descargas de nutrientes nesta região, podendo servir de base para análises nos restantes sistemas de afloramento costeiro de fronteira oriental. Este conjunto de sistemas de *upwelling*, apesar das suas diferenças, já estudadas, na disponibilidade de nutrientes, na produtividade primária e nas próprias características do afloramento costeiro, sabe-se que têm em comum a predominância de comunidades de diatomáceas e condições de limitação em azoto semelhantes. Como tal, as respostas da comunidade de fitoplâncton considerada neste estudo podem ser similares às observadas nestes sistemas de afloramento costeiro, particularmente nos casos em que possa ocorrer limitação em ferro, como o sistema de afloramento costeiro da Corrente da Califórnia.

TABLE OF CONTENTS

ACKNOWLEDGEMENTS	I
ABSTRACT	III
RESUMO ALARGADO	IV
TABLE OF CONTENTS	VII
LIST OF TABLES	VIII
LIST OF FIGURES	IX
LIST OF ABBREVIATIONS AND SYMBOLS	XIII
1. INTRODUCTION	1
1.1. State of the art	1
1.2. Aim and objectives	6
2. METHODS	7
2.1. Study site	7
2.2. Seawater sample collection	8
2.3. Experimental design	8
2.4. Nutrient Analysis	10
2.5. Phytoplankton community analysis	10
2.5.1. Cell abundances analysis	10
2.5.2. HPLC analysis	10
2.5.3. CHEMTAX Analysis	11
3. RESULTS	12
3.1. Pre-experiment environmental conditions	12
3.2. Chlorophyll and nutrients dynamics	14
3.3. Nitrogen-to-phosphorus ratio	16
3.4. Phytoplankton Community	17
4. DISCUSSION	27
4.1. Post-bloom phytoplankton response to nutrient enrichment	27
4.2. Phytoplankton response to nutrient enrichment: Additional pulses	29
4.3. <i>Chaetoceros</i> dominance	30
4.4. Changes in pigment and photoacclimation	31
4.5. Final considerations	33
REFERENCES	33

LIST OF TABLES

Table 2.1: Stock solution composition for each experimental treatment.	9
Table 2.2: Measured and target (in brackets) concentrations for DIN (dissolved inorganic nitrogen) and phosphate on Day 0.....	9
Table 2.3: Detected phytoplankton pigments concentrations throughout the experiment (mean and minimum-maximum values)	10
Table 2.4: Initial and final pigments-to-chl a ratio matrices in CHEMTAX analysis.	11
Table 3.1: Cell abundances (mean and minimum-maximum values) of the 10 most abundant taxa observed.....	19

LIST OF FIGURES

- Figure 1.1: SNPP VIIRS mean sea surface temperature (SST) for 2015. The rectangles signal the location of the four Eastern Boundary Upwelling Systems (EBUS). 2
- Figure 1.2: Relationship between the nitrate uptake pathway (highlighted by the green dotted line) and photosynthesis during periods of low temperature and high nitrate concentration. Nitrate reductase (NR); Nitrite reductase (NiR); Dissolved organic nitrogen (DON); light energy (hv); PSII (photosystem II), e⁻ (electrons), RUBISCO (Ribulose-1,5-bisphosphate carboxylase/oxygenase); PGA (phosphoglyceric acid). Adapted from Lomas and Glibert (1999a). a). 4
- Figure 1.3: A) Succession of phytoplankton communities as nutrients and turbulence decrease (Mandala; Margalef, 1978). B) Succession of phytoplankton communities as nutrients and turbulence decrease (main sequence) and alternative sequence that leads to red tide events, showing main groups associated with each state (Margalef et al., 1979). C) Separation of phytoplankton life-strategies (C, R and S) as a result of the interaction between nutrient accessibility and light depth (Reynolds, 1987). 4
- Figure 1.4: Revision of Margalef's mandala, including 12 traits of marine phytoplankton. The traits are: 1) the gradient of nitrogen forms preferentially assimilated, from ammonium to nitrate and/or from organic to inorganic forms; 2) the gradient of the dissolved inorganic N/P ratio; 3) the gradient of adaptation to high vs low light and autotrophy vs mixotrophy; 4) the gradient of the cell's motility, from absence of motility to swimming to strategies of vertical sink/float migration; 5) the gradient of turbulence from low to high; 6) the gradient of pigmentation of cells, through the relative proportion of pigments classes; 7) the gradient of temperature from high to low; 8) the gradient of cell size, from small to large; 9) the gradient of the phytoplankton's growth rate, from low to high; 10) the gradient of the tendency of cells to be toxic or to produce other bioreactive compounds, from high to low; 11) the ecological strategy gradient, ranging from r to K and 12) propensity for the resulting production to constitute regenerated production or new production (Glibert, 2016)..... 5
- Figure 2.1: The Humboldt Current System (HCS), with special emphasis on the Central Chile region (30°-40°S). Main upwelling centres are represented by black dots, while grey dots represent sites with frequent upwelling. Coastal areas with occasional upwelling are shown as dark lines. Adapted from Thiel et al., 2007..... 7
- Figure 2.2: Location (red triangle) of the seawater sample collection off Algarrobo Bay, Chile. 8
- Figure 3.1: SNPP VIIRS mean sea surface temperature (SST; °C) and chlorophyll a concentration (CHL; mg m⁻³) in the Chilean coast on the weeks preceding the experiment (on the left: 9th-16th, on the right: 16th-23th of October 2013). The red triangle marks the location of the water collection station. 12
- Figure 3.2: Mean WindSat wind vector direction and speed (ms⁻¹) in the South-East Pacific on

the weeks preceding the experiment (12th-19th and 19th-26th of October 2013). The red triangle marks the location of the water collection station. Note that the three round black patches on the left side of the images correspond to the Desventuradas and Juan Fernández archipelagoes. 13

Figure 3.3: Mean chlorophyll a concentrations (mg.m⁻³) from Day 0 to Day 6 for both treatments and control. Error bars shown are standard errors (SE). Note that the dotted, dashed and solid lines respectively correspond to Control, N-limited and P-limited values... 14

Figure 3.4: Dissolved inorganic nitrogen (NO₂⁻ + NO₃⁻) mean concentrations (μM) from Day 0 to Day 6 for both treatments and control. Error bars shown are standard errors (SE). Note that the dotted, dashed and solid lines respectively correspond to Control, N-limited and P-limited values. 15

Figure 3.5: Phosphate (PO₄³⁻) mean concentrations (μM) from Day 0 to Day 6 for both treatments and control. Error bars shown are standard errors (SE). Note that the dotted, dashed and solid lines respectively correspond to Control, N-limited and P-limited values... 15

Figure 3.6: Mean nitrogen-to-phosphorus ratio (N:P) from Day 0 to Day 6 for both treatments and control. Error bars shown are standard errors (SE). Note that the dotted, dashed and solid lines respectively correspond to Control, N-limited and P-limited values. 16

Figure 3.7: Mean total cell abundances (cells L⁻¹) from Day 0 to Day 6 for both treatments and control. Error bars shown are standard errors (SE). Note that the dotted, dashed and solid lines respectively correspond to Control, N-limited and P-limited values. 17

Figure 3.8: Mean cell abundances (cells L⁻¹) of pennate diatoms (solid line with dark squares), centric diatoms (solid line with white circles), phytoflagellates (Chrysophyceae + Cryptophyceae + Prasinophyceae + Prymnesiophyceae + Euglenophyceae; dotted line with white triangles) and dinoflagellates (dash-dotted line with white diamonds) in the Control treatment. Error bars shown are standard errors (SE). 18

Figure 3.9: Mean cell abundances (cells L⁻¹) of pennate diatoms (solid line with dark squares), centric diatoms (solid line with white circles), phytoflagellates (Chrysophyceae + Cryptophyceae + Prasinophyceae + Prymnesiophyceae + Euglenophyceae; dotted line with white triangles) and dinoflagellates (dash-dotted line with white diamonds) in the N-limited treatment. Error bars shown are standard errors (SE). 18

Figure 3.10: Mean cell abundances (cells L⁻¹) of pennate diatoms (solid line with dark squares), centric diatoms (solid line with white circles), phytoflagellates (Chrysophyceae + Cryptophyceae + Prasinophyceae + Prymnesiophyceae + Euglenophyceae; dotted line with white triangles) and dinoflagellates (dash-dotted line with white diamonds) in the P-limited treatment. Error bars shown are standard errors (SE). 19

Figure 3.11: Mean cell abundances (cells L⁻¹) of Chaetoceros sp. (dash-dotted line with black diamonds), Nitzschia sp. (solid line with white triangle), Gymnodinium sp. (dotted line with black square) and Scrippsiella sp. (dashed line with white circle) in the N-limited treatment. Error bars shown are standard errors (SE). 20

Figure 3.12: Mean cell abundances (cells L⁻¹) of Chaetoceros sp. (dash-dotted line with black

diamonds), *Nitzschia* sp. (solid line with white triangle), *Gymnodinium* sp. (dotted line with black square) and *Scrippsiella* sp. (dashed line with white circle) in the P-limited treatment. Error bars shown are standard errors (SE). 21

Figure 3.13: Total chlorophyll a (TChl a; dashed line with black squares) and chlorophyll a degradation products - chlorophyllide a (Chlide a; dotted line with white diamonds), pheophytin a (Phe a; solid line with white circles) and pheophorbide a (Pheide a; grey line with grey triangles) mean concentrations (mg m^{-3}) from Day 0 to Day 6 in the Control treatment. Error bars shown are standard errors (SE). Note that pheophorbide a concentrations are measured in the secondary axis (right, in gray). 22

Figure 3.14: Total chlorophyll a (TChl a; dashed line with black squares) and chlorophyll a degradation products - chlorophyllide a (Chlide a; dotted line with white diamonds), pheophytin a (Phe a; solid line with white circles) and pheophorbide a (Pheide a; grey line with grey triangles) mean concentrations (mg m^{-3}) from Day 0 to Day 6 in the N-limited treatment. Error bars shown are standard errors (SE). Note that pheophorbide a concentrations are measured in the secondary axis (right, in gray). 22

Figure 3.15: Total chlorophyll a (TChl a; dashed line with black squares) and chlorophyll a degradation products - chlorophyllide a (Chlide a; dotted line with white diamonds), pheophytin a (Phe a; solid line with white circles) and pheophorbide a (Pheide a; grey line with grey triangles) mean concentrations (mg m^{-3}) from Day 0 to Day 6 in the P-limited treatment. Error bars shown are standard errors (SE). Note that pheophorbide a concentrations are measured in the secondary axis (right, in gray). 23

Figure 3.16: Mean concentrations (mg m^{-3}) of MgDVP (solid line with white squares), chlorophyll c_2 (Chl c_2 ; dotted line with white circles), fucoxanthin (Fuco; dashed line with grey triangles), chlorophyll b (Chl b; dash-dotted line with white circles) and chlorophyll a (Chl a; dotted line with black diamonds) from Day 0 to Day 6 in the N-limited treatment. Error bars shown are standard errors (SE). 23

Figure 3.17: Mean concentrations (mg m^{-3}) of MgDVP (solid line with white squares), chlorophyll c_2 (Chl c_2 ; dotted line with white circles), fucoxanthin (Fuco; dashed line with grey triangles), chlorophyll b (Chl b; dash-dotted line with white circles) and chlorophyll a (Chl a; dotted line with black diamonds) from Day 0 to Day 6 in the N-limited treatment. Error bars shown are standard errors (SE). 24

Figure 3.18: Chlorophyll a concentrations (absolute contribution; mg m^{-3}), estimated through the CHEMTAX analysis, for Haptophyceae (Hapto), dinoflagellates (Dinof), Chrysophyceae (Chryso) and diatoms from Day 0 to Day 6 in the N-limited treatment. Error bars shown are standard errors (SE). 24

Figure 3.19: Chlorophyll a concentrations (absolute contribution; mg m^{-3}), estimated through the CHEMTAX analysis, for Haptophyceae (Hapto), dinoflagellates (Dinof), Chrysophyceae (Chryso) and diatoms from Day 0 to Day 6 in the P-limited treatment. Error bars shown are standard errors (SE). 25

Figure 3.20: CHEMTAX chlorophyll a absolute concentrations (mg m^{-3}) obtained through CHEMTAX for diatoms against diatoms abundances (cells L^{-1}) for both experimental

treatments.	25
Figure 3.21: CHEMTAX chlorophyll a absolute concentrations (mg m^{-3}) obtained through CHEMTAX for dinoflagellates against dinoflagellates abundances (cells L^{-1}) for both experimental treatments.	26
Figure 3.22: CHEMTAX chlorophyll a absolute concentrations (mg m^{-3}) obtained through CHEMTAX for diatoms against diatoms abundances (cells L^{-1}), only for Days 1 and 2, for both experimental treatments.	26
Figure 3.23: CHEMTAX chlorophyll a absolute concentrations (mg m^{-3}) obtained through CHEMTAX for dinoflagellates against dinoflagellates abundances (cells L^{-1}), only for Days 1 and 2, for both experimental treatments.	27

LIST OF ABBREVIATIONS AND SYMBOLS

β,β – Car	β,β -Carotene
Chl <i>a</i>	Chlorophyll <i>a</i>
Chl <i>b</i>	Chlorophyll <i>b</i>
Chl <i>c</i> ₂	Chlorophyll <i>c</i> ₂
Chl <i>c</i> ₃	Chlorophyll <i>c</i> ₃
Chlide <i>a</i>	Chlorophyllide <i>a</i>
DIN	Dissolved Inorganic Nitrogen
EBUS	Eastern Boundary Upwelling Systems
FAO	Food and Agriculture Organization of the United Nations
Fuco	Fucoxanthin
HCS	Humboldt Current System
Hex-fuco	19'-Hexanoyloxyfucoxanthin
HPLC	High Performance Liquid Chromatography
MgDVP	Mg-2,4-divinylpheoporphyrin <i>a</i> ₅ monomethyl ester
N:P	Nitrogen-to-Phosphorus Ratio
NH ⁴⁺	Ammonium
NO ₂ ⁻	Nitrite
NO ₃ ⁻	Nitrate
OSPAR	Convention for the Protection of the Marine Environment of the North-East Atlantic
Phe <i>a</i>	Pheophytin <i>a</i>
Pheide <i>a</i>	Pheophorbide <i>a</i>
PO ₄ ³⁻	Phosphate
PTFE	Polytetrafluoroethylene
Si[OH] ₄	Silicic acid
SNPP VIIRS	Suomi National Polar-Orbiting Partnership Visible Infrared Imaging Radiometer Suite
SST	Sea Surface Temperature
TChl <i>a</i>	Total Chlorophyll <i>a</i> (Chlorophyll <i>a</i> + epimer + allomer)

1. INTRODUCTION

1.1. State of the art

The occurrence of nutrient enrichment in coastal areas may have different sources and, in severe cases, can lead to serious disturbances in marine ecosystems (Smith et al., 1999). Eutrophication is frequently considered as potentially harmful for aquatic ecosystems and able to disrupt ecosystem services. However, for truly understanding eutrophication, it is crucial to separate the process from its causes and consequences (Nixon, 1995).

Eutrophication can occur naturally or due to anthropogenic forcing, but it is always driven by enrichment in nutrients (Ferreira et al., 2011). Human-induced or cultural eutrophication is commonly associated with land-originated inputs, originating from point (e.g. wastewater effluent, runoff from mines or aquacultures, waste disposal sites or animal feedlots) or non-point sources (e.g. atmospheric deposition or runoff from agriculture or urbanization; Carpenter et al., 1998). This enrichment in nutrients can prompt a significant increase in the biomass of primary producers, leading to a decrease in transparency and to an increase in organic matter sedimentation. In severe cases of eutrophication, this situation may deteriorate as high consumption of oxygen from both grazers and sediment aerobic bacteria leads to oxygen depletion and, consequently, to mass death of fish and macroinvertebrates (Ferreira et al., 2011).

When eutrophication initially began to be widely regarded as a problem circa 1960s (Nixon, 1995), scientists initially thought of it as a state. For instance, Rodhe (1969) created a classification system for determining eutrophication in lakes that considered its primary production. In this system, a lake with $350\text{-}700\text{ g C m}^{-2}\text{ year}^{-1}$ was classified as eutrophic (in a polluted sense). Over the past few decades, however, some authors have argued that eutrophication should be rather seen as a process (e.g. Ansari et al., 2011; Ferreira et al., 2011; Nixon, 1995). During this period, the definition of eutrophication has been intensively discussed. Nixon (1995), searching for an operational definition, defined it as “an increase in the rate of supply of organic matter to an ecosystem”. However, this definition was deemed as insufficient for water quality management and, after further discussion, more adequate definitions emerged. For instance, the OSPAR Eutrophication Strategy defines it as the “enrichment of water by nutrients causing an accelerated growth of algae and higher forms of plant life to produce an undesirable disturbance to the balance of organisms present in the water and to the quality of the water concerned, and therefore refers to the undesirable effects resulting from anthropogenic enrichment by nutrients (...)” (OSPAR Commission, 2010). This and other similar definitions have been imperative for the implementation of environmental legislation that tackles eutrophication, such as the Marine Strategy Framework Directive (Directive 2008/56/EC; e.g. Cabrita et al., 2015; Ferreira et al., 2011; Fleming-Lehtinen et al., 2015)

Natural eutrophication occurs due to natural processes, for example due to natural nutrient flow from rivers or upwelling. However, it should be noted that, nowadays, most rivers are highly influenced by anthropogenic action and that pristine rivers are scarce. In most cases, this sort of eutrophication is considered as an important part of the natural variability of a given aquatic system. Coastal upwelling occurs when deep nutrient-rich and cooler waters arise as winds drive alongshore, enhancing primary productivity (Thiel et al., 2007). This phenomenon is particularly important in four major coastal currents located in the eastern boundaries of the Pacific and Atlantic basins, the eastern boundary current systems (EBUS; Figure 1.1): the California Current System (CalCS), the Canary Current System (CanCS), the Humboldt Current System (HCS) and the Benguela Current System (BCS). Despite covering less than 2% of the ocean, these systems are responsible for 7% of the global marine primary production and more than 20% of global fish catches (Wang et al., 2015).

Notwithstanding their common upwelling occurrence, these systems are highly heterogeneous and there are differences in the timing, duration and intensity of the upwelling. For instance, in lower latitudes, upwelling can occur all year, while in higher latitudes it displays a seasonal pattern, occurring mainly during spring and summer (Wang et al., 2015).

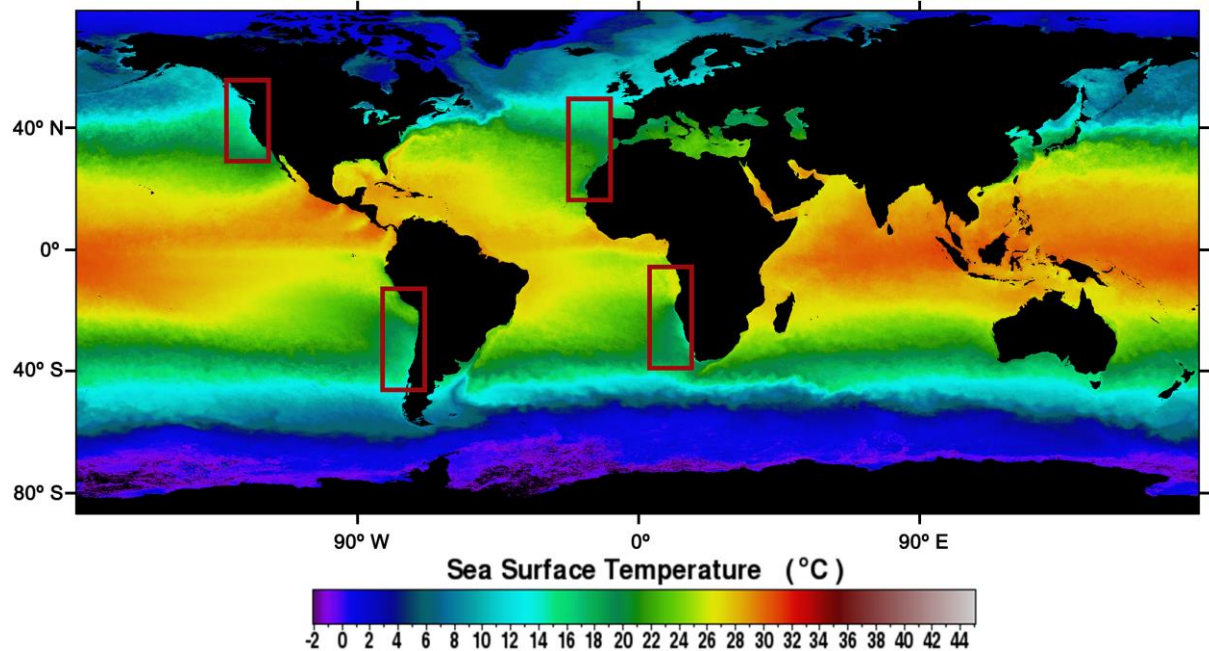


Figure 1.1: SNPP VIIRS mean sea surface temperature (SST) for 2015. The rectangles signal the location of the four Eastern Boundary Upwelling Systems (EBUS).

The Humboldt Current System extends from $\sim 42^{\circ}\text{S}$ up to the equator (Thiel et al., 2007) and encompasses the shoreline along Chile, Peru and Equador. Due to its heterogeneity, the HCS can be divided in three biomes: i) the upwelling system off Peru ($\sim 4\text{-}16^{\circ}\text{S}$), known for its immense productivity and upwelling occurrence during all year, ii) the moderate to low productivity zone from southern Peru to northern Chile ($18\text{-}26^{\circ}\text{S}$) and iii) central Chile ($30\text{-}40^{\circ}\text{S}$), typical of seasonal upwelling and high productivity (Chavez and Messié, 2009). Despite displaying one the highest average primary productivities of all the EBUS ($2.18 \text{ g C m}^{-2} \text{ day}^{-1}$; Carr, 2002), its active area is smaller than BCS and CalCS, thus contributing to a lower annual primary productivity than its counterparts (Carr, 2002). Nonetheless, the HCS is one of the regions with highest fish production (representing 10% of the world fish catch; Chavez et al., 2008), particularly due to the well-known anchoveta (*Engraulis ringens* Jenyns, 1842) fishery off coastal Peru, whose landings from 2003-2012 averaged over 7 million tonnes (FAO, 2016). This production is due to the HCS's unique efficiency in the energy transfer between trophic levels (Chavez and Messié, 2009), leading to a much higher fish per unit of primary production. Thus, as its main primary producers, phytoplankton communities have a major role in the maintaining the functioning of the HCS.

Marine phytoplankton communities can be very diverse, encompassing a myriad of life forms which may range from $0.2 \mu\text{m}$ to over 2 mm (Reynolds, 2006). For phytoplankton, apart from cell size (i.e. width), the surface-to-volume (S/V) ratio is also considered as a relevant trait for phytoplankton physiology. The higher the S/V ratio is, the easier it is for cells to assimilate nutrients and grow faster (Reynolds, 2006). The S/V ratio has direct implications on the constant of half saturation (K_s , i.e. the concentration of a given nutrient required to satisfy half of the maximum uptake capacity of the cell). Thus, smaller phytoplanktons with high S/V ratios and low K_s , such as cyanobacteria and small

flagellates (e.g. most Chrysophyceae, Cryptophyceae and Haptophyceae), can grow under lower nutrient conditions.

Photosynthesis is a process common to most primary producers in nature. In general, this process utilizes electromagnetic radiation as an energy source, carbon is fixed and oxygen is released. Photosynthesis is essential for the production of organic compounds (through the synthesis of organic carbon from inorganic carbon), converting light energy into chemical energy. Since photosynthesis cannot occur without light, phytoplankton is not able to grow under light limitation. However, living near the surface, where light intensity may be excessive, can result in photoinhibition and damage of cells' photosystems. Thus, most phytoplankton generally live in an intermediate layer, called the deep chlorophyll maximum (DCM), where there exists an optimization of the utilization of light and nutrients. In fact, sustained phytoplankton growth is only possible if the concentration of nutrients in the surrounding waters is sufficient. For phytoplankton, the nutrients most often associated with growth limitation are nitrogen (N) and phosphorus (P), as both are essential for important internal components of the cell like nucleic acids (Reynolds, 2006). However, there are other elements that may act as limiting nutrients, such as iron (Fe), due to its important role as an electron acceptor in photosynthesis, and silicon (Si). Silicon, along with oxygen and hydrogen, makes up silicic acid ($\text{Si}(\text{OH})_4$), an important component for the skeleton (frustule) of diatoms. Thus, silicon limitation may occur and inhibit diatom growth.

Nutrient requirements by phytoplankton have been extensively studied in the past. Redfield (1934, 1958) discovered that carbon, nitrate and phosphate concentrations observed in different oceans occurred in the same proportions (C:N:P = 106:16:1). He also concluded that the exact same proportions could be generally found in phytoplankton cells. This ratio, known as the Redfield ratio, is still used nowadays because of its importance for understanding ocean biogeochemistry. Later, the Redfield ratio was extended to include iron (C:N:P:Fe = 106:16:1:0.001; Sarmiento & Gruber, 2006) and silicon (C:Si:N:P = 106:15:16:1; Brzezinski, 1985) due to their role as possible limiting nutrients.

These nutrients can be available in both its inorganic or organic forms, but are generally assimilated by phytoplankton in its inorganic form. Inorganic nitrogen, for instance, is mainly available to phytoplankton in the form of the ions nitrate (NO_3^-), nitrite (NO_2^-) and ammonium (NH_4^+). Of these three forms, nitrate is the most common in the open sea, hence being the one that is typically assimilated by phytoplankton (Reynolds, 2006). This status can change in coastal regions due to the influence of multiple inputs. Nonetheless, nitrate must be reduced to ammonium in order to be utilized intracellularly (Owens and Esaias, 1976; Figure 1.2). This process requires additional metabolic energy cost, which is why ammonium was, until recently, thought as the preferentially assimilated inorganic nitrogen compound for all phytoplankton groups (Dortch, 1990).

In spite of this theoretical disadvantage in assimilating nitrate, several studies have shown that diatom assemblages under low temperatures ($<15^\circ\text{C}$) and high concentrations of nitrate favour nitrate assimilation (Glibert et al., 2015; Lomas and Glibert, 1999a, b). Under such conditions, diatoms are highly productive and generate electrons in excess from photosynthesis. In order to avoid photoinhibition of photosynthesis, cells have to dissipate some of these electrons through the reduction of nitrate (via nitrate reductase; see Figure 1.2). Thus, they hypothesized that nitrate assimilation is a strategy to maintain intracellular energy balance. This is particularly relevant for understanding the dynamics of diatoms in upwelling-influenced ecosystems given that low temperatures and high nitrate concentrations are typical of these regions.

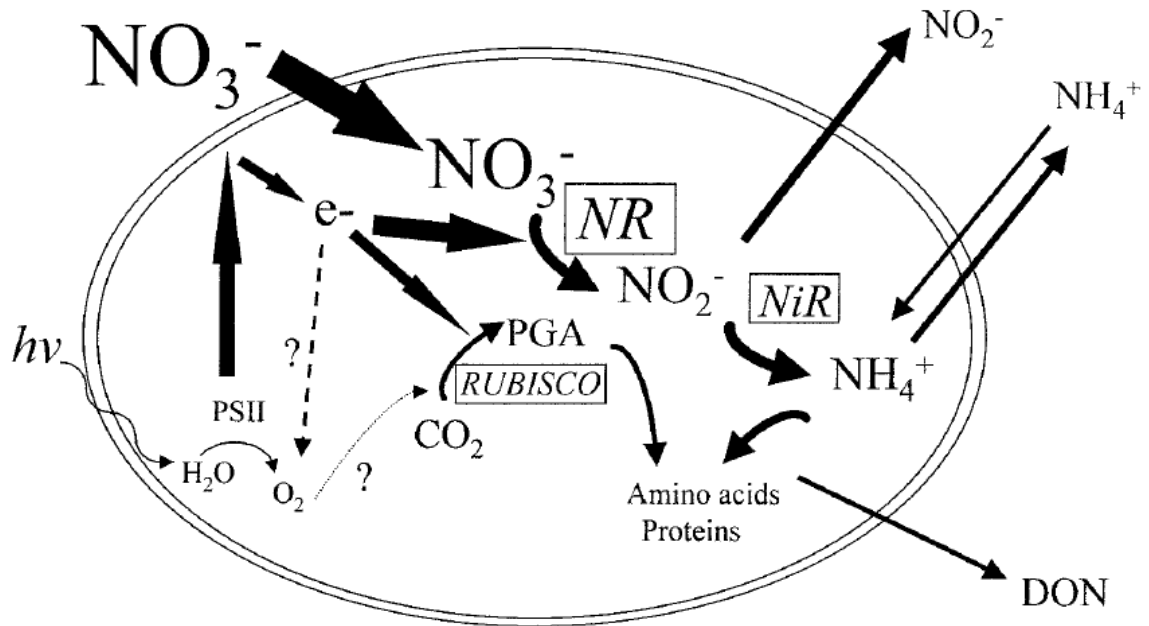


Figure 1.2: Relationship between the nitrate uptake pathway and photosynthesis during periods of low temperature and high nitrate concentration. Nitrate reductase (NR); Nitrite reductase (NiR); Dissolved organic nitrogen (DON); light energy ($h\nu$); PSII (photosystem II), e^- (electrons), RUBISCO (Ribulose-1,5-bisphosphate carboxylase/oxygenase); PGA (phosphoglyceric acid). Adapted from Lomas and Glibert (1999a). a).

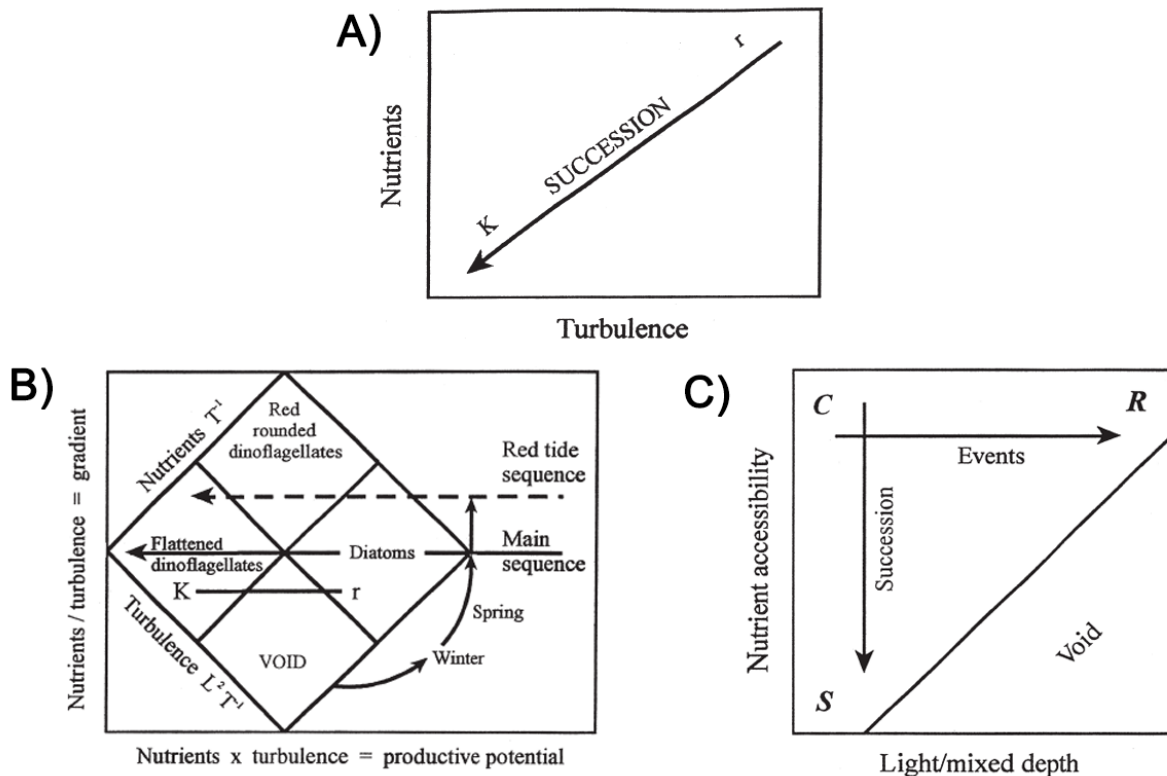


Figure 1.3: A) Succession of phytoplankton communities as nutrients and turbulence decrease (Mandala; Margalef, 1978). B) Succession of phytoplankton communities as nutrients and turbulence decrease (main sequence) and alternative sequence that leads to red tide events, showing main groups associated with each state (Margalef et al., 1979). C) Separation of phytoplankton life-strategies (C, R and S) as a result of the interaction between nutrient accessibility and light depth (Reynolds, 1987).

However, it is not just light and nutrients that determine phytoplankton growth and ecology. Turbulence is also very important in shaping phytoplankton assemblages. In 1978, Margalef introduced his “mandala”, clarifying the underlying relation between turbulence and nutrient availability (Figure 1.3A). According to Margalef, turbulence, unless when excessive, could help the uptake of nutrients and assure the survival of non-motile populations, like most diatoms. In such an environment, motility would be regarded as a waste of energy. However, the less turbulent an environment is, the more essential motility becomes to avoid sinking and consequent cell losses, which is why dinoflagellates dominate stratified waters. The “mandala” successfully simplified this succession from r species (i.e. species that thrive under unstable environments, such as diatoms) to K species (i.e. typically associated with stable environments, such as dinoflagellates) in a typical temperate winter-spring bloom sequence. Later, Margalef tried to explain the formation of red tides as a divergence from the main succession promoted by nutrient inputs from terrestrial and anthropogenic sources (Margalef et al., 1979; Figure 1.3B).

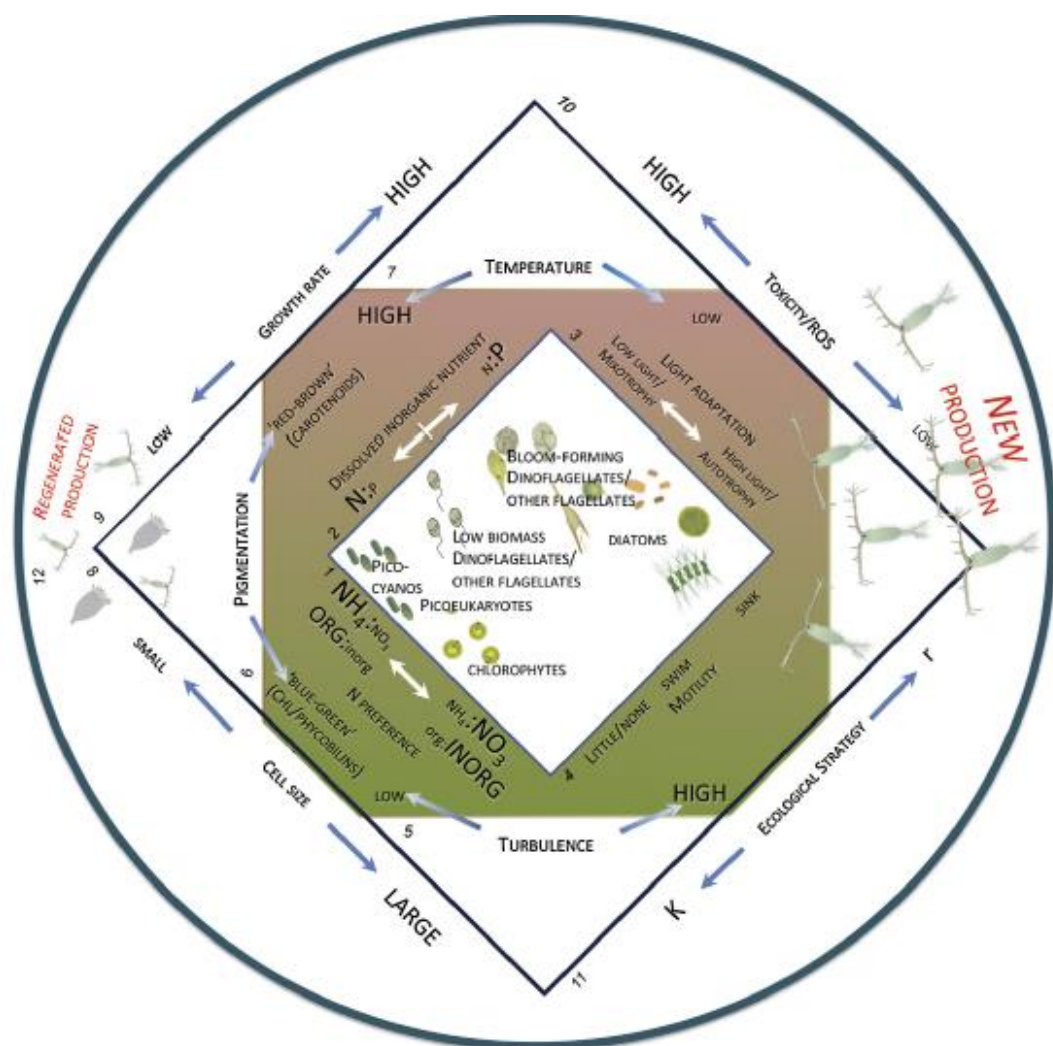


Figure 1.4: Revision of Margalef’s mandala, including 12 traits of marine phytoplankton. The traits are: 1) the gradient of nitrogen forms preferentially assimilated, from ammonium to nitrate and/or from organic to inorganic forms; 2) the gradient of the dissolved inorganic N/P ratio; 3) the gradient of adaptation to high vs low light and autotrophy vs mixotrophy; 4) the gradient of the cell’s motility, from absence of motility to swimming to strategies of vertical sink/float migration; 5) the gradient of turbulence from low to high; 6) the gradient of pigmentation of cells, through the relative proportion of pigments classes; 7) the gradient of temperature from high to low; 8) the gradient of cell size, from small to large; 9) the gradient of the phytoplankton’s growth rate, from low to high; 10) the gradient of the tendency of cells to be toxic or to produce other bioactive compounds, from high to low; 11) the ecological strategy gradient, ranging from r to K and 12) propensity for the resulting production to constitute regenerated production or new production (Glibert, 2016).

The subject of phytoplankton life-strategies was again addressed by Reynolds in his “*intaglio*”, a conceptual model that divided phytoplankton into colonists (C-strategists), slow-growers (S-strategist) and ruderals (R-strategists) (Reynolds, 1987; Smayda and Reynolds, 2001; Figure 1.3C). This model differed from the Margalef’s mandala in some aspects: i) it originally focused on freshwater phytoplankton (although it has since been applied to marine waters, e.g. Alves-de-Souza et al., 2008; Brito et al., 2015); ii) each of the three adaptive strategy (C, S and R) may include r- or K-selected species and iii) it adapts the mandala’s nutrients and turbulence axes to nutrient accessibility and light/mixed depth, respectively. More recently, Margalef’s mandala was expanded by Glibert (2016), resulting in a highly complex updated mandala which covers twelve effects or response traits, such as the ecological strategy (r or K), temperature, cell size and relative availability of inorganic nitrogen or phosphorus (see Glibert, 2016 for more details; Figure 1.4). In this new mandala, diatoms are shown to be associated with, for example, high turbulence, low temperatures, higher concentrations of nitrate and nitrogen limitation. Another conclusion is that bloom-forming dinoflagellates are more associated with nitrogen limitation, low temperatures and higher growth rates than low biomass dinoflagellates. These models are crucial for understanding phytoplankton dynamics in an ever-changing world.

Changes in environmental conditions can lead to changes in phytoplankton communities. As seen above, light, nutrient availability and turbulence or stratification have implications on the phytoplanktonic groups that bloom and dominate an ecosystem. Since any given change in the community might have consequences for the ecosystem, particularly in the local trophic chain, the dominance of a particular phytoplankton group may determine which organisms top the trophic web. Cury (2008) demonstrated such dynamic in marine trophic webs off Cape Agulhas. On one hand, when turbulence is low, phytoflagellates dominate. These are then consumed by small copepods, which in turn are consumed by sardines. On the other hand, diatoms bloom when turbulence is high and are consumed by larger copepods. These larger copepods are preferentially consumed by anchovies. Thus, there is a natural oscillation between high biomasses of sardines or anchovies.

There is still much to learn about how phytoplankton communities react to nutrient enrichments, whether these enrichments are natural or anthropogenic. This knowledge would be essential for providing insight on their implications for the ecosystem functioning. Thus, solving this challenge would be the first step towards the possibility of assessing the potential impacts of changes in environmental conditions, namely nutrient availability. One crucial way is through laboratory experiments with natural phytoplankton assemblages. Despite its intrinsic limitations (Carpenter, 1996; Schindler, 1987), these experiments are one of the best tools available to understand phytoplankton dynamics and its relation with nutrients inputs (Domingues et al., 2015).

1.2. Aim and objectives

The main goal of this study is to understand the response of phytoplankton communities to pulse nutrient enrichments in a region of intense upwelling conditions. To achieve this goal, several specific objectives were established: i) assess the biomass response to known nutrient pulses; ii) study the succession of the phytoplankton community under enrichment; iii) examine if the phytoplankton community reacts differently to nutrient pulses with distinct compositions; iv) analyse if the complementary use of a chemotaxonomy approach (HPLC-CHEMTAX) can provide additional valuable insight.

2. METHODS

2.1. Study site

The coastal waters off Central Chile (30-40°S; Figure 2.1) are one of the main biomes of the Humboldt Current System. Upwelling in this region displays a seasonal recurrent pattern, occurring during the austral spring-summer (October-March), when favourable winds (from S/SW) predominate (Thiel et al., 2007). Due to the high spatial heterogeneity of the coastline, upwelling is more intense in the following locations: off Coquimbo (30°S), off Valparaíso (33°S) and off Concepción (36°S). These upwelling centres contribute to a high productivity during upwelling season and are the major reason why Chile became one of the main “fishing nations”, with high abundance of sardines and anchovies’ stocks (Peterson et al., 1988). The mean upwelling intensity in Central Chile is high ($\sim 1.2 \text{ m}^2 \text{ s}^{-1}$), but is considerably lower than other intense upwelling regions (e.g. $>2 \text{ m}^2 \text{ s}^{-1}$ off Peru and off Namibia; PFEL upwelling index, Wang et al., 2015). However, it is also much higher than what can be found off the Iberian Peninsula ($<1 \text{ m}^2 \text{ s}^{-1}$; Wang et al., 2015), per example. During upwelling season, chlorophyll a ranges between $3.8\text{-}26 \text{ mg m}^{-3}$, much higher values than what have been measured during winter ($1\text{-}2.5 \text{ mg m}^{-3}$; González et al. 1989; Montecino et al. 2004).

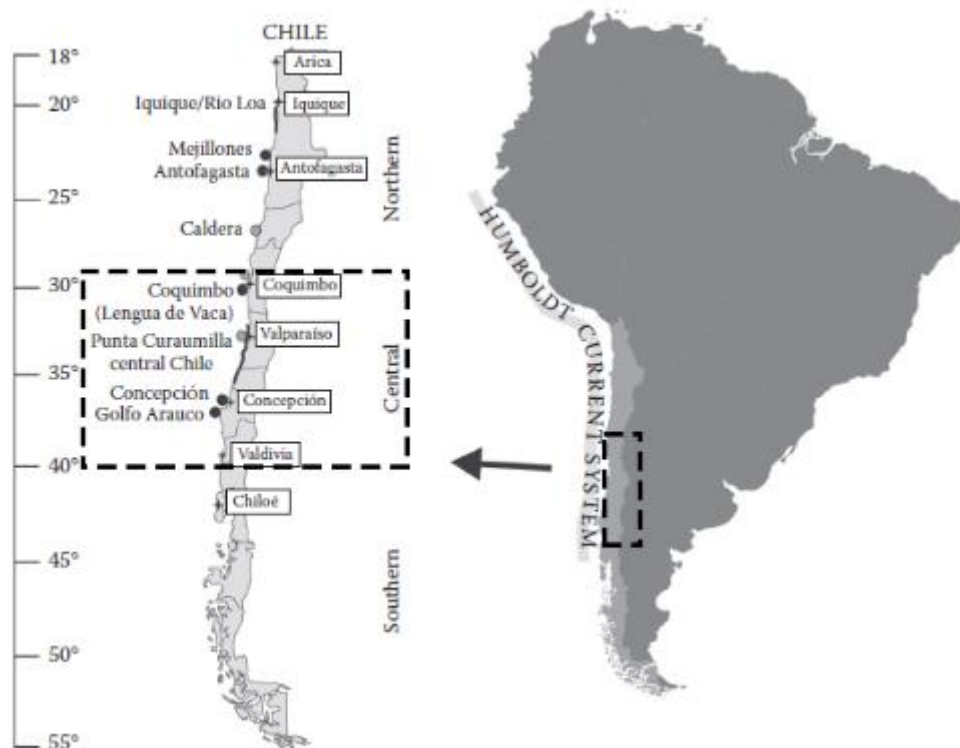


Figure 2.1: The Humboldt Current System (HCS), with special emphasis on the Central Chile region (30°-40°S). Main upwelling centres are represented by black dots, while grey dots represent sites with frequent upwelling. Coastal areas with occasional upwelling are shown as dark lines. Adapted from Thiel et al., 2007.

This region has relatively low average sea surface temperature (SST; e.g. 14°C off Valparaíso; Hormazabal et al., 2001), mainly due to the Humboldt Current upward transport of nutrient-rich cooler subantarctic waters and, in the austral summer, to strong upwelling. However, this dynamic can be interrupted during El Niño events. When these events occur, warm and nutrient-poor equatorial waters are conveyed to coastal Chile, interrupting the flow of the Humboldt Current. This leads to a general increase in SST and, consequently, a decrease in upwelling intensity in the region. Moreover, it can

cause negative impacts on the local communities (Thiel et al., 2007). One of the main characteristics of this region is the occurrence of iron limitation during intense upwelling events. This trait is common in the HCS, mostly due to its short continental shelf and low riverine influence, the main sources of iron in coastal waters (Hutchins et al., 2002; Thiel et al., 2007).

2.2. Seawater sample collection

Seawater was collected on the 25th October of 2013, at noon, from a coastal point facing the Algarrobo Bay in the Valparaíso region, Chile ($33^{\circ}19'16.9''\text{S}$ $71^{\circ}45'36.3''\text{W}$; Figure 2.2). Niskin bottles were used to collect approximately 200 L of seawater from the surface (0-5 m depth). Seawater was then filtered through a 200 μm mesh in order to remove zooplankton, macroalgae and detritus.

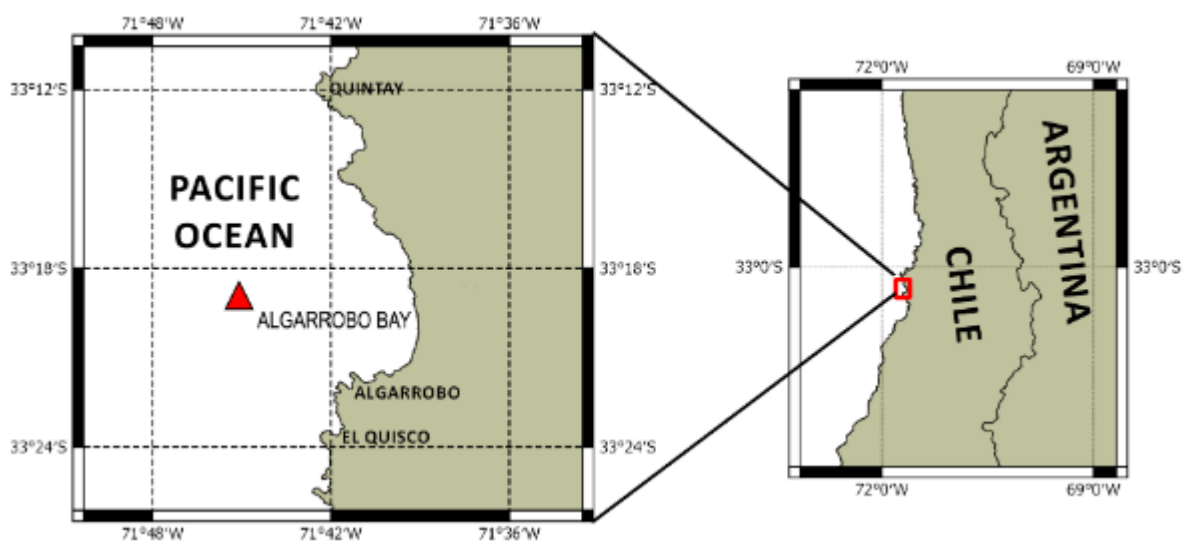


Figure 2.2: Location (red triangle) of the seawater sample collection off Algarrobo Bay, Chile.

The seawater was then rapidly transported in 50L jerricans to the laboratory in the Estación Costera de Investigaciones Marinas “Las Cruces” (ECIM; $33^{\circ}30'05.8''\text{S}$ $71^{\circ}38'01.7''\text{W}$), where it was agitated to ensure homogenisation and partitioned into plastic containers, the microcosms/incubators used in these experiments. The containers were acid-washed and rinsed with natural seawater for 3 times to ensure that no contamination, particularly nutrients, was taking place. They were subsequently filled with 3 L and allowed to rest in a tank with regular light conditions until the following day.

2.3. Experimental design

In order to assess the response of the phytoplankton community to different nutrient enrichments, two different experimental treatments were established: the N-limited and the P-limited treatments. In each treatment, the microcosms were enriched with a solution containing nitrate (NO_3^-) and phosphate (PO_4^{3-}), specifically prepared to achieve those conditions, using the N:P Redfield ratio as a benchmark (N-limited = $\text{N:P} < 16:1$; P-limited = $\text{N:P} > 16:1$; Redfield, 1958). Both solutions also contained silicic acid ($\text{Si}[\text{OH}]_4$) to prevent Si-limitation. These solutions were prepared with analytical grade NaNO_3 , NaH_2PO_4 and Na_2SiO_3 reagents (Table 2.1), thus only altering the reactants' ratio to reach the adequate nutrient final concentrations. The recipes chosen for achieving each of these solutions followed previous works by Brito (2010), Brito et al., (2010) and Edwards et al. (2003,

2001). A control treatment was also established.

Table 2.1: Stock solution composition for each experimental treatment and target concentrations in the microcosms (in brackets)

Treatment	Reactant	Nutrient concentration in stock solution (µM)
N-limited	NaNO ₃ (Ji and Sherrell, 2008)	770.88 (12.0)
	NaH ₂ PO ₄ · H ₂ O (Ji and Sherrell, 2008)	115.63 (1.8)
	Na ₂ SiO ₃ · 9H ₂ O	1927.19 (30.0)
P-limited	NaNO ₃ (Ji and Sherrel, 2008)	1927.19 (30.0)
	NaH ₂ PO ₄ · H ₂ O (Ji and Sherrel, 2008)	12.85 (0.2)
	Na ₂ SiO ₃ · 9H ₂ O	1927.19 (30.0)

The experiment started on the 26th of October 2013 (Day 0). Containers were manually agitated 4 times per day and temperature and salinity were monitored everyday with the help of a thermometer and a refractometer, respectively, to make sure these conditions remained stable throughout the experiments.

2.2.1. Experiment details

The experiment focused on phytoplankton response to pulse enrichment events, simulated in laboratory by two separate microcosm enrichments. These enrichments occurred at day 0 and at day 3, halfway through the experiment.

Table 2.2 displays the initial post-enrichment nutrients concentrations. 24 microcosms (12 per treatment) were subjected to both treatments considered previously: N-limited and P-limited. Another 12 containers were used as controls. From day 0 to day 6, two containers (plus one control) from each treatment were sacrificed every day. Sacrificed containers were used for the measurement of nutrients and phytoplankton pigments and for microscopic analysis of the phytoplankton community. This approach prevented any interference with the ongoing experiment, avoiding any contamination to the incubators. The enrichment was done by adding 47.6 mL of the solution associated with each treatment (Table 2.2). The added volume was the same for each treatment to avoid any issues related to dilution factors. The second enrichment pulse, on day 3, was intended to assess how the community reacted to an enrichment event shortly after the other. The experiment ended in day 6, when the last microcosms were removed.

Table 2.2: Measured and target (in brackets) concentrations for DIN (dissolved inorganic nitrogen) and phosphate on Day 0.

Treatment	Nutrient concentration (µM)	
	DIN	Phosphate
Control	0.8	1.0
N-limited	13.0 (12.0)	2.9 (1.8)
P-limited	30.8 (30.0)	1.2 (0.2)

Note: Control's nutrient concentrations correspond to the measured concentrations in natural seawater and therefore should be regarded as the surplus found regarding the targets concentrations.

2.4. Nutrient Analysis

A sample of 200 mL was collected from each sacrificed incubator, frozen immediately at -25°C and subsequently analysed to measure dissolved inorganic nutrients (nitrate and nitrite ($\text{NO}_2^- + \text{NO}_3^-$), phosphate (PO_4^{3-}) and silicic acid ($\text{Si}[\text{OH}]_4$) with the aid of a AutoAnalyzer, accordingly to the methodology of Atlas et al. (1971). The analyses were carried out at the Pontificia Universidad Católica de Valparaíso. Nitrogen-to-phosphorus ratio (N:P) was calculated since it significantly influences the phytoplankton species composition (Tilman et al., 1982).

2.5. Phytoplankton community analysis

2.5.1. Cell abundances analysis

Samples (125 mL) were taken from the sacrificed containers and subsequently preserved with neutral Lugol's solution (2%). Samples were then kept in brown-glass flasks and stored in a cool place. Before the analysis, 100 mL settling chambers were used for 48 hours after gently agitating the samples for homogenisation. Phytoplankton cells were counted and identified to the lowest taxon possible (Lund et al., 1958; Utermöhl, 1958) using an inverted light microscope, in agreement with the proceedings of Chrétiennot-Dinet (1990), Hoppenrath et al. (2009), Ricard (1987), Sournia (1986) and Tomas (1997).

2.5.2. HPLC analysis

300 mL samples were filtered with Whatman GF/F glass fibre filters (25 mm diameter and $0.7\ \mu\text{m}$ pore size) in low light conditions. After filtration, filters were stored at -80°C until analysis. In order to extract phytoplankton pigments, the filters were placed in centrifuge tubes for extraction in 3 mL of 95% cold-buffered methanol (2% ammonium acetate), containing the pigment trans- β -Apo-8'-carotenal ($0.05\ \text{mg L}^{-1}$ as the internal standard). Samples were then sonicated (Bransonic 1210) for 5 minutes, placed in the freezer (-20°C) and allowed to rest for one hour. Following 5 min centrifugation at 3°C , the extract was filtered through PTFE membrane filters ($0.2\ \mu\text{m}$ pore size) to ensure that no residues were inserted in the HPLC system. For pigment analyses, Zapata et al. (2000) method was carried out with a $1\ \text{ml min}^{-1}$ flux and an injection volume of $100\ \mu\text{l}$. This method uses a monomeric C8 column and a mobile phase containing pyridine. After pigment identification from absorbance spectra and retention times, concentrations were calculated from signals in the photodiode array detector. Pigment standards from DHI (Institute for Water and Environment, Denmark) were used to previously calibrate the HPLC.

Table 2.3: Detected phytoplankton pigments concentrations throughout the experiment (mean and minimum-maximum values)

Abbreviation	Pigment	Average and range of concentrations (mg m^{-3})
Chl <i>a</i>	Chlorophyll <i>a</i>	0.206 (0.000-1.889)
TChl <i>a</i>	Total Chlorophyll <i>a</i>	0.279 (0.000-2.549)
Chlide <i>a</i>	Chlorophyllide <i>a</i>	0.042 (0.000-0.589)
Chl <i>b</i>	Chlorophyll <i>b</i>	0.054 (0.000-0.136)
Chl <i>c</i> ₂	Chlorophyll <i>c</i> ₂	1.247 (0.061-3.949)
Chl <i>c</i> ₃	Chlorophyll <i>c</i> ₃	0.065 (0.000-0.205)
Diadino	Diadinoxanthin	0.010 (0.000-0.095)

Fuco	Fucoxanthin		0.331 (0.000-2.343)
Hex-fuco	19'-Hexanoyloxyfucoxanthin		0.026 (0.000-0.079)
MgDVP	Mg-2,4-divinylpheoporphyrin monomethyl ester	a5	0.139 (0.000-0.925)
Pheide a	Pheophorbide a		11.916 (1.603-31.821)
Phe a	Pheophytin a		0.132 (0.000-0.533)
$\beta\beta$ - Car	β,β -Carotene		0.002 (0.000-0.051)

2.5.3. CHEMTAX Analysis

The CHEMTAX chemical taxonomy software (version 1.95; Mackey et al., 1996; Wright et al., 1996) was used to estimate the relative contribution of phytoplankton groups to total chlorophyll *a* biomass, hence calculating their relative abundances. This software, given an initial pigment ratio matrix, uses factor analysis and a steepest descent algorithm to calculate the best fit to the data acquired through HPLC, as shown in Mackey et al. (1996).

Four phytoplankton classes were considered (Diatoms-1, Dinoflagellates-4, Chrysophyceae and Haptophyceae) based on identified pigments (HPLC) and main taxa from microscopy. The pigments chosen were chl *c*₃, fucoxanthin, hex-fuco (19' – hexanoyloxyfucoxanthin), chl *b* and chl *a* and its initial pigment ratios to chlorophyll *a* were obtained from previous several CHEMTAX studies (diatoms-1 - Gibb et al., 2001; dinoflagellates-4 - Lampert et al., 2016; Chrysophyceae - Laza-Martinez et al., 2007; Haptophyceae - Seoane et al., 2009). The relatively low number of pigments loaded into the software is a result of the low pigment variability in the collected water sample (Table 2.). Diatoms-1 were included due to the detection of high abundances of *Chaetoceros sp.* Dinoflagellates-4 inclusion was prompted by the presence of *Gymnodinium sp.* cells and the absence of peridinin, while Chrysophyceae were the most abundant flagellate group in microscopy samples. Pigment data was divided in two sub-matrices (N-limited and P-limited) according to which treatment the samples were subjected. These sub-matrices did not include any control samples as it would increase the error, thus affecting the CHEMTAX analysis. The initial and final ratios are shown in.

Table 2.4: Initial and final pigments-to-chl *a* ratio matrices in CHEMTAX analysis.

Taxa	Chl <i>c</i> ₃	Fuco	Hex-fuco	Chl <i>b</i>	Chl <i>a</i>
Initial ratios					
Diatoms-1	0	0,818	0	0	1
Dinoflagellates-4	0	0	0	0,741	1
Chrysophyceae	0,250	0,970	0	0	1
Haptophyceae	0,229	0,316	0,534	0	1
Final ratios (N-limited)					
Diatoms-1	0	0,727	0	0	1
Dinoflagellates-4	0	0	0	0,738	1
Chrysophyceae	0,522	0,271	0	0	1
Haptophyceae	0,128	0,208	0,424	0	1
Final ratios (P-limited)					
Diatoms-1	0	0,637	0	0	1
Dinoflagellates-4	0	0	0	0,730	1
Chrysophyceae	0,498	0,285	0	0	1
Haptophyceae	0,127	0,215	0,428	0	1

In order to optimize the CHEMTAX analysis, 60 pigment ratios matrices were generated by multiplying each cell of the initial ratio matrix by a randomly determined factor (Wright et al., 2009). The final matrix consisted in the average of the six ratio output matrices with lowest residual or root

mean square errors (< 0.05), thereby obtaining the best results. All the analyses were done following the proceedings of Wright et al. (2009).

3. RESULTS

3.1. Pre-experiment environmental conditions

Sea surface temperature, as measured by the SNPP VIIRS mission, for the two weeks preceding the experiment near the water collection station was between 12° - 14° C (Figure 3.1), similar values to the 14° C measured in the Day 0 sample. The low SST detected along the Chilean Western coast are typical of a coastal upwelling event, a pattern which is corroborated by high chlorophyll *a* values in the same time-period. Plus, Figure 3.2 displays upwelling-favourable winds recorded near the sampling station with speed ranging from 5-10 m/s.

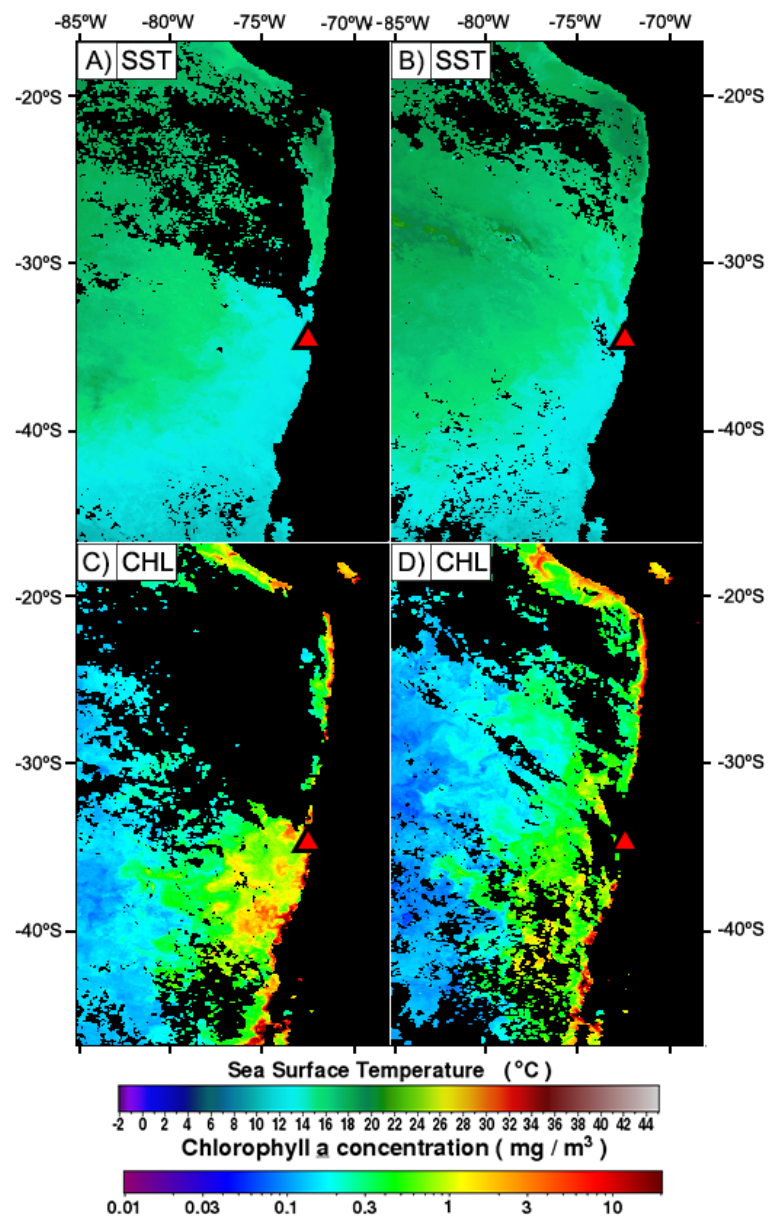


Figure 3.1: SNPP VIIRS mean sea surface temperature (SST; $^{\circ}$ C) and chlorophyll *a* concentration (CHL; mg m^{-3}) in the Chilean coast on the weeks preceding the experiment (on the left: 9th-16th, on the right: 16th-23th of October 2013). The red triangle marks the location of the water collection station.

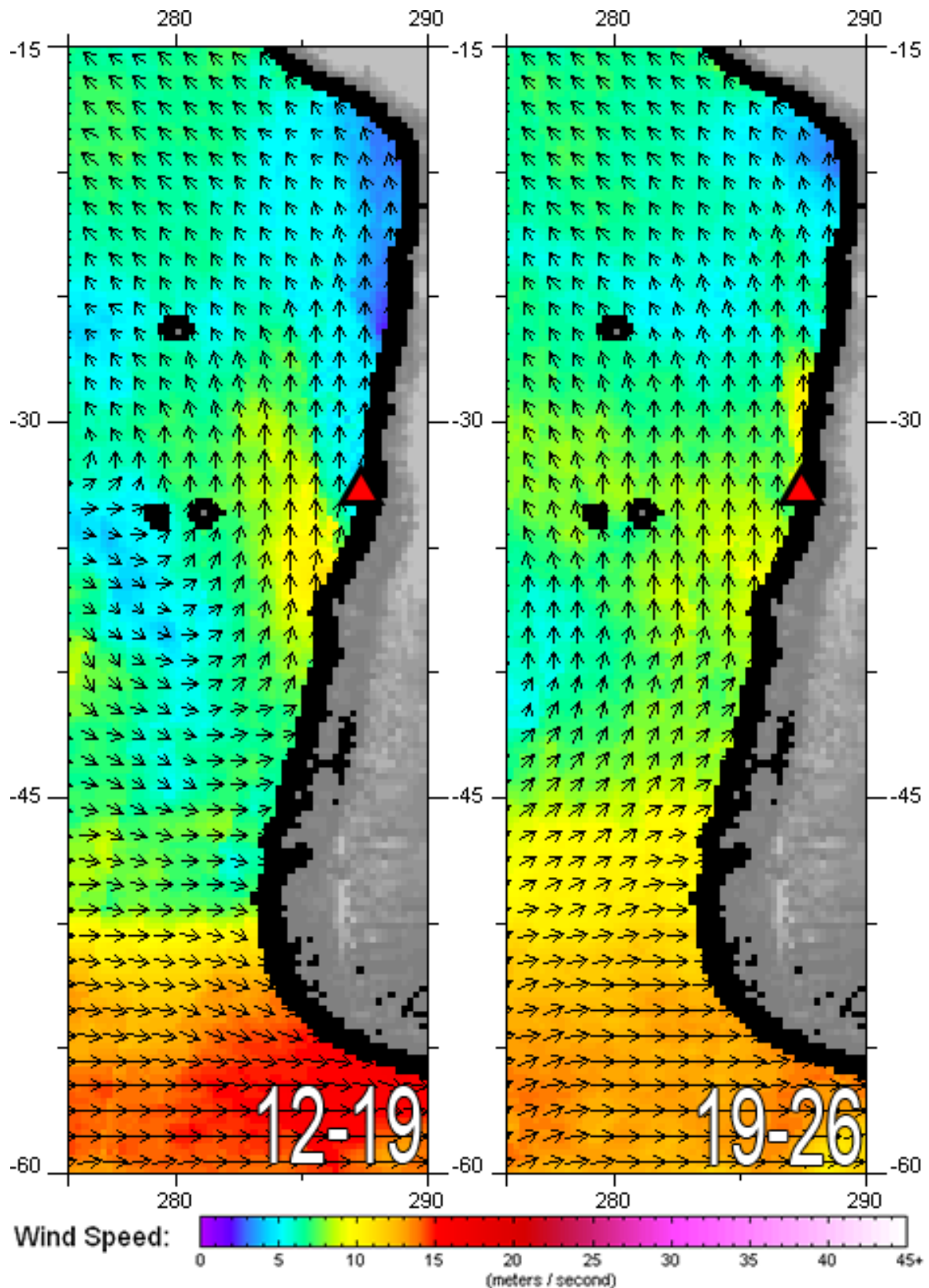


Figure 3.2: Mean WindSat wind vector direction and speed (ms^{-1}) in the South-East Pacific on the weeks preceding the experiment (12th-19th and 19th-26th of October 2013). The red triangle marks the location of the water collection station. Note that the three round black patches on the left side of the images correspond to the Desventuradas and Juan Fernández archipelagoes.

Thus, the environmental conditions gathered suggest upwelling occurrence, particularly in the week of 9th-16th October (Figure 3.1). Nutrient-rich waters due to upwelling are generally limited in nitrogen (i.e. with low N/P ratios), a view which is supported by the measured N/P ratio in Day 0 (0.83).

3.2. Chlorophyll and nutrients dynamics

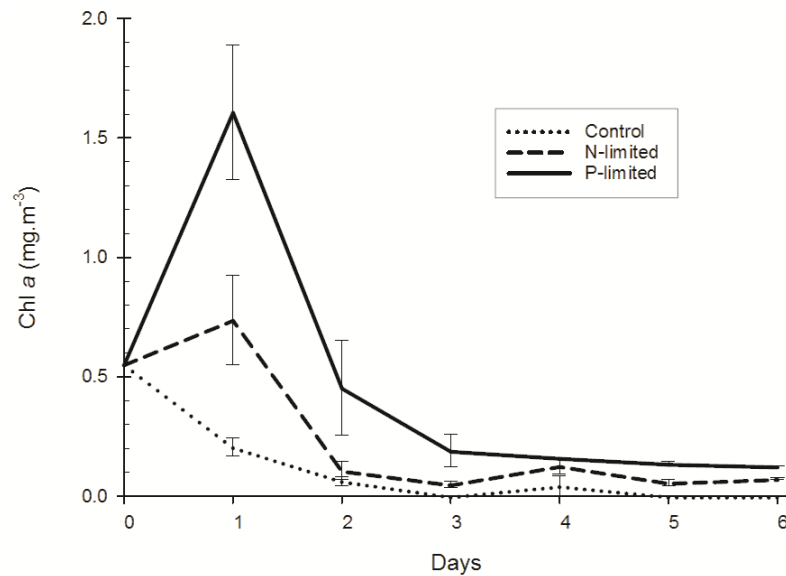


Figure 3.3: Mean chlorophyll *a* concentrations (mg.m⁻³) from Day 0 to Day 6 for both treatments and control. Error bars shown are standard errors (SE). Note that the dotted, dashed and solid lines respectively correspond to Control, N-limited and P-limited values.

Both treatments triggered an increase in chlorophyll *a* after the initial enrichment, reaching maximum chl *a* concentrations on Day 1 (Figure 3.3). Chl *a* values in the P-limited treatment (1.61 mg m⁻³) were more than twice as high as the measured in the N-limited (0.74 mg m⁻³), also on Day 1. After Day 1, chlorophyll *a* decreased throughout the experiment. The only exception was after the second enrichment pulse (Day 3) in the N-limited treatment, where a small peak (0.13 mg m⁻³) was registered. In the P-limited treatment, no chl *a* increase occurred after the second enrichment event. Contrastingly, chlorophyll *a* values in control samples dropped on Day 1 and remained low. Despite showing a similar trend throughout the experiment, chlorophyll *a* concentrations were always higher in the P-limited treatment, particularly in the first days.

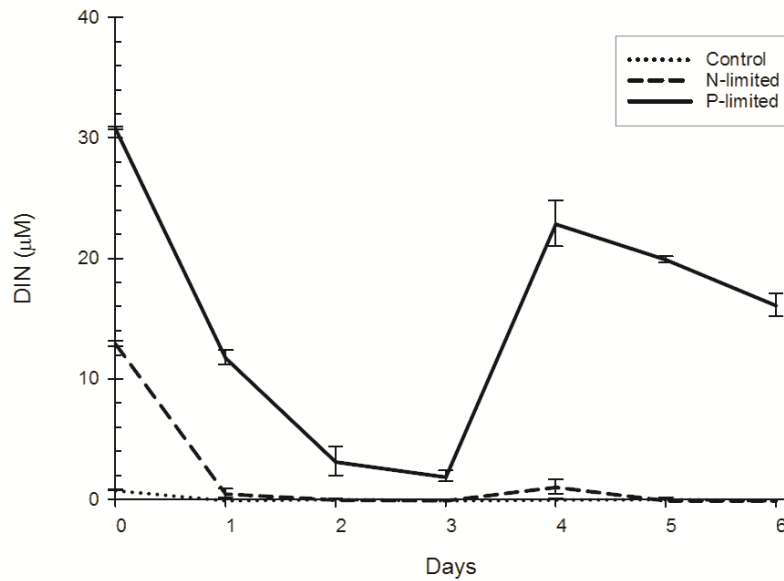


Figure 3.4: Dissolved inorganic nitrogen ($\text{NO}_2^- + \text{NO}_3^-$) mean concentrations (μM) from Day 0 to Day 6 for both treatments and control. Error bars shown are standard errors (SE). Note that the dotted, dashed and solid lines respectively correspond to Control, N-limited and P-limited values.

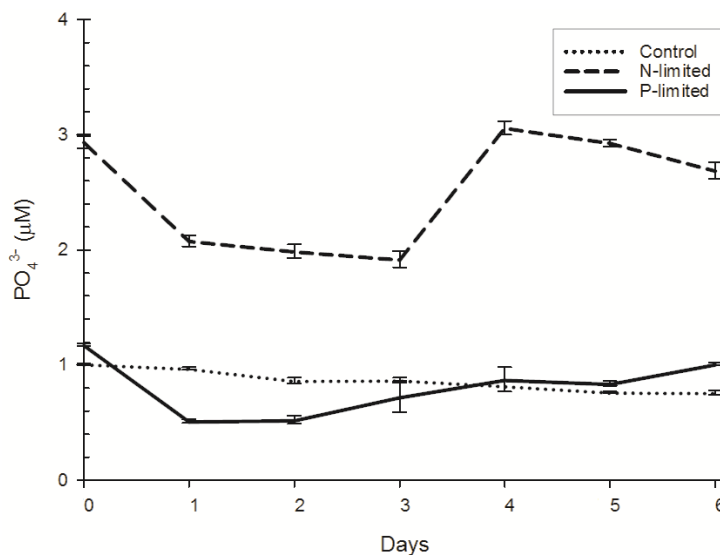


Figure 3.5: Phosphate (PO_4^{3-}) mean concentrations (μM) from Day 0 to Day 6 for both treatments and control. Error bars shown are standard errors (SE). Note that the dotted, dashed and solid lines respectively correspond to Control, N-limited and P-limited values.

DIN and phosphate concentrations, for both treatments, are shown in Figures 3.4 and 3.5. In the P-limited treatment, nitrate concentrations sharply decreased from the beginning of the experiment until it reached a minimum of $1.95 \mu\text{M}$ on Day 3. After the second enrichment stage, it increased to $22.9 \mu\text{M}$ on Day 4 and then started to drop again. Meanwhile, in the N-limited treatment, almost all nitrogen was consumed after Day 0. This condition remained constant until the end of the experiment, even though there was a minor peak ($1.1 \mu\text{M}$) on Day 4. Regarding phosphate, its concentration in the N-limited treatment slowly rose to $1.01 \mu\text{M}$ after a 44% decline on Day 1. However, its behaviour in the N-limited treatment was similar to the one shown by nitrate in the P-limited: a decrease on Day 1 followed by an increase after Day 3, when the enrichment pulse occurred. Yet, in this case, phosphate reached a maximum of $3.06 \mu\text{M}$ on Day 4.

Overall, DIN concentrations were considerably higher in the P-limited treatment than in the N-limited, where they were kept within low values due to higher nitrogen consumption than enrichment. Moreover, phosphate did not appear to have been consumed as much in the P-limited. Its concentration kept slowly rising after Day 1 in the P-limited treatment while nitrate was being consumed. DIN and phosphate concentrations in control samples remained low with a slight decrease and did not fluctuate. When comparing nutrient concentrations against chlorophyll *a* (Figure 3.3), it seems phytoplankton did not respond to the second enrichment pulse despite Figures 3.4 and 3.5 showing nitrate and phosphate consumption over that period.

3.3. Nitrogen-to-phosphorus ratio

The N/P ratios measured in the experiment are shown in Figure 3.6. As N-limited treatment samples were mainly enriched in phosphate, nitrogen-to-phosphorus ratios registered in the N-limited treatment and in the control samples were, as expected, low, remaining below 0.4 after the experiment began (Day 1).

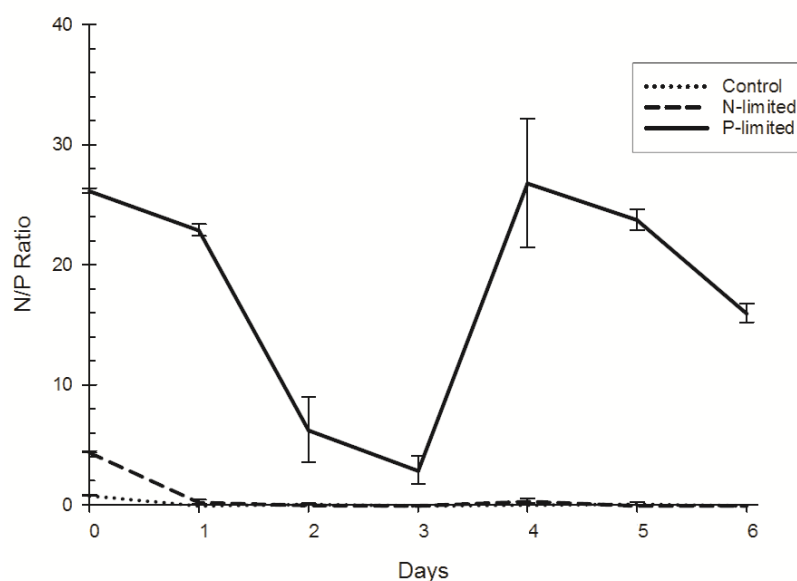


Figure 3.6: Mean nitrogen-to-phosphorus ratio (N:P) from Day 0 to Day 6 for both treatments and control. Error bars shown are standard errors (SE). Note that the dotted, dashed and solid lines respectively correspond to Control, N-limited and P-limited values.

In the P-limited treatment, despite the initial high N/P ratio (26.18), it rapidly fell to 2.91 on Day 3. After rising to 26.82 on Day 4 due to the second enrichment pulse, the N/P ratio started to decline again and reached 15.98 in the end of the experiment. Overall, N:P appeared to have a tendency for nitrogen limitation values (<16.0; Redfield, 1958), even when originally limited in phosphorus.

3.4. Phytoplankton Community

Figure 3.7 shows phytoplankton cells abundance time series for all treatments. In both treatments, abundance peaked on Day 1 and declined after it. In the P-limited treatment, concentrations increased again on Day 3 and reached a maximum of 16.9×10^6 cells L^{-1} on Day 4. From Day 4-6, abundance decreased to 10.9×10^6 cells L^{-1} . In the N-limited treatment though, the response to the second enrichment was clearer as cells abundance only increased on Day 4 (16.0×10^6 cells L^{-1}). Higher abundances were always found in the P-limited treatment (predominantly N enrichment). Cells abundances seem to confirm the initial increase in biomass already seen in chlorophyll *a* concentrations. However, cell abundance peaked in the second half of the experiment, showing an increase in biomass that is inconsistent with chl *a* data.

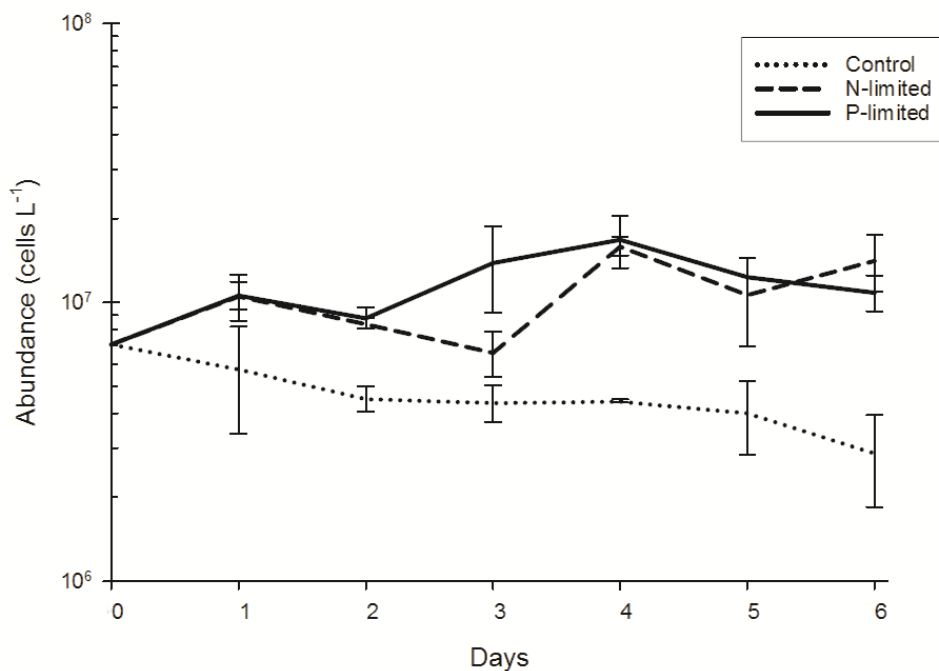


Figure 3.7: Mean total cell abundances (cells L^{-1}) from Day 0 to Day 6 for both treatments and control. Error bars shown are standard errors (SE). Note that the dotted, dashed and solid lines respectively correspond to Control, N-limited and P-limited values.

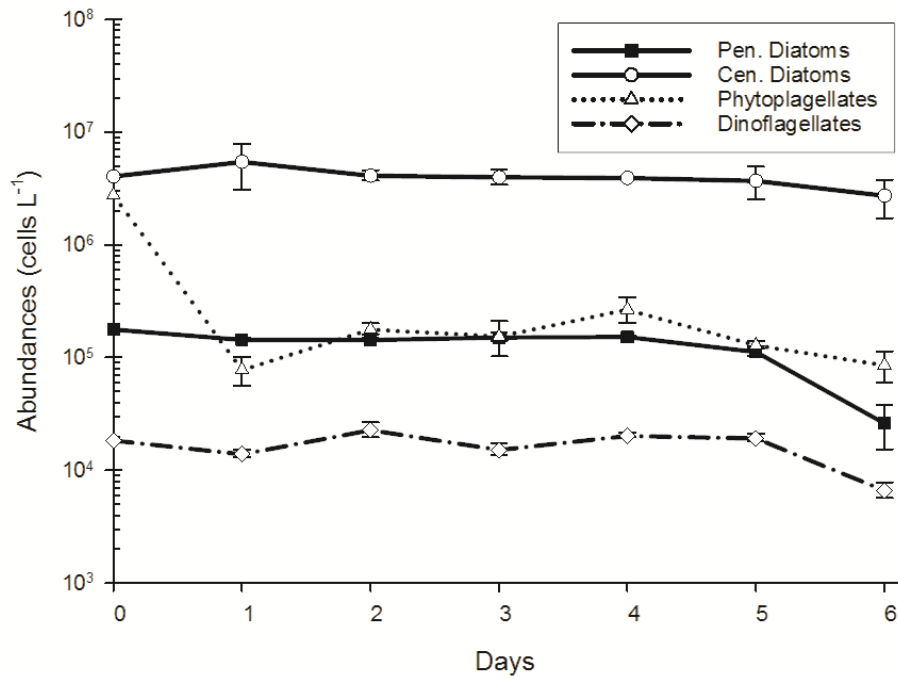


Figure 3.8: Mean cell abundances (cells L⁻¹) of pennate diatoms (solid line with dark squares), centric diatoms (solid line with white circles), phytoflagellates (Chrysophyceae + Cryptophyceae + Prasinophyceae + Prymnesiophyceae + Euglenophyceae; dotted line with white triangles) and dinoflagellates (dash-dotted line with white diamonds) in the Control treatment. Error bars shown are standard errors (SE).

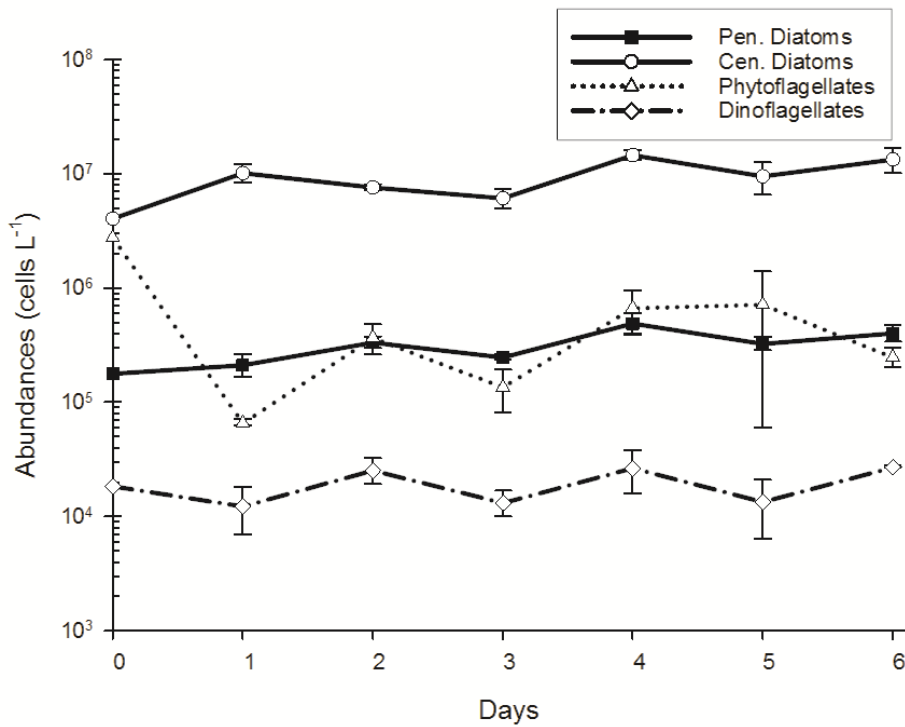


Figure 3.9: Mean cell abundances (cells L⁻¹) of pennate diatoms (solid line with dark squares), centric diatoms (solid line with white circles), phytoflagellates (Chrysophyceae + Cryptophyceae + Prasinophyceae + Prymnesiophyceae + Euglenophyceae; dotted line with white triangles) and dinoflagellates (dash-dotted line with white diamonds) in the N-limited treatment. Error bars shown are standard errors (SE).

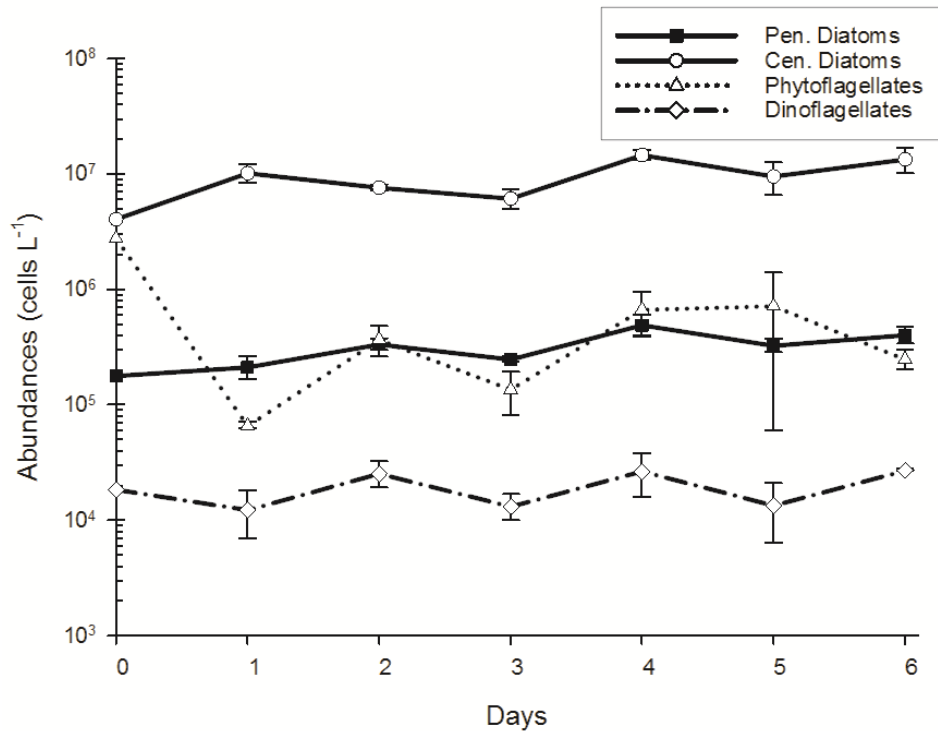


Figure 3.10: Mean cell abundances (cells L⁻¹) of pennate diatoms (solid line with dark squares), centric diatoms (solid line with white circles), phytoflagellates (Chrysophyceae + Cryptophyceae + Prasinophyceae + Prymnesiophyceae + Euglenophyceae; dotted line with white triangles) and dinoflagellates (dash-dotted line with white diamonds) in the P-limited treatment. Error bars shown are standard errors (SE).

The phytoplankton community on Day 0 was mainly composed of centric diatoms (57.7%) and phytoflagellates (39.4%) – calculated as the sum of species of the classes Chrysophyceae, Cryptophyceae, Prasinophyceae, Prymnesiophyceae and Euglenophyceae. However, after the experiment began, centric diatoms abundance increased while flagellates decreased, resulting in a community dominated by centric diatoms. For instance, centric diatoms made up 97% (~10.3 × 10⁶ cells L⁻¹) of total phytoplankton cells on Day 1 in both experimental treatments (Figures 3.9 and 3.10). This trend was observed throughout the experiment, regardless of the treatment, as it was also observed in control samples (Figure 3.8). On Day 4, centric diatoms abundance reached a maximum of 15.6 × 10⁶ cells L⁻¹ in the P-limited and of 14.7 × 10⁶ cells L⁻¹ in the N-limited treatments. Focusing solely on the remaining phytoplankton groups, phytoflagellates and pennate diatoms combined cells abundances amounted to an average ~6% of the community from Day 1-6 in both treatments while dinoflagellates made up just ~0.17% (17.9 × 10³ cells L⁻¹) in average. A quick comparison between phytoflagellates numbers in both treatments revealed that phytoflagellates appeared in higher percentages in the N-limited treatment than in the P-limited one (+15.1% in average).

Table 3.1: Cell abundances (mean and minimum-maximum values) of the 10 most abundant taxa observed.

Taxa	Average and range of abundances (× 10 ³ cells L ⁻¹)
Bacillariophyceae	
<i>Asterionellopsis glacialis</i>	40.4 (2.4-111.0)
<i>Chaetoceros sp.</i>	8 305.4 (1699.6-18 908.0)
<i>Cylindrotecha closterium</i>	20.0 (0.7-63.2)

<i>Dactyliosolen sp.</i>	13.8 (0.0-63.2)
<i>Nitzschia sp.</i>	191.7 (11.7-448.0)
<i>Skeletonema sp.</i>	110.5 (5.6-622.0)
Chrysophyceae	187.2 (0.0-1600.0)
Cryptophyceae	89.3 (0.0-1000.0)
Dinophyceae	
<i>Gymnodinium sp.</i>	5.0 (0.0-16.0)
<i>Scripsiella sp.</i>	8.1 (1.2-18.4)

A detailed analysis of species data revealed very high abundances of *Chaetoceros sp.* ($\sim 8.3 \times 10^6$ in average). Apart from this taxon, other diatoms species belonging to the genera of *Nitzschia*, *Skeletonema*, *Cylindrotecha*, *Dactyliosolen* and *Asterionellopsis* were frequently identified. Dinoflagellates were mostly composed of *Scripsiella sp.* and *Gymnodinium sp.* Abundance data of several of these taxa are shown in Figures 3.11 and 3.12 and in Table 3.1. Although cell numbers of taxa *Chaetoceros sp.* and *Nitzschia sp.* remained somewhat constant, *Scripsiella sp.* and *Gymnodinium sp.* fluctuated throughout the experiment. Compared to diatoms, dinoflagellates were present in low numbers as seen by *Gymnodinium sp.* (5.0×10^3 cells L^{-1} in average) and *Scripsiella sp.* (8.1×10^3 cells L^{-1} in average) abundances. Between Day 1-6, *Chaetoceros sp.* cells made up roughly 92% (in average) of the community in the microcosms.

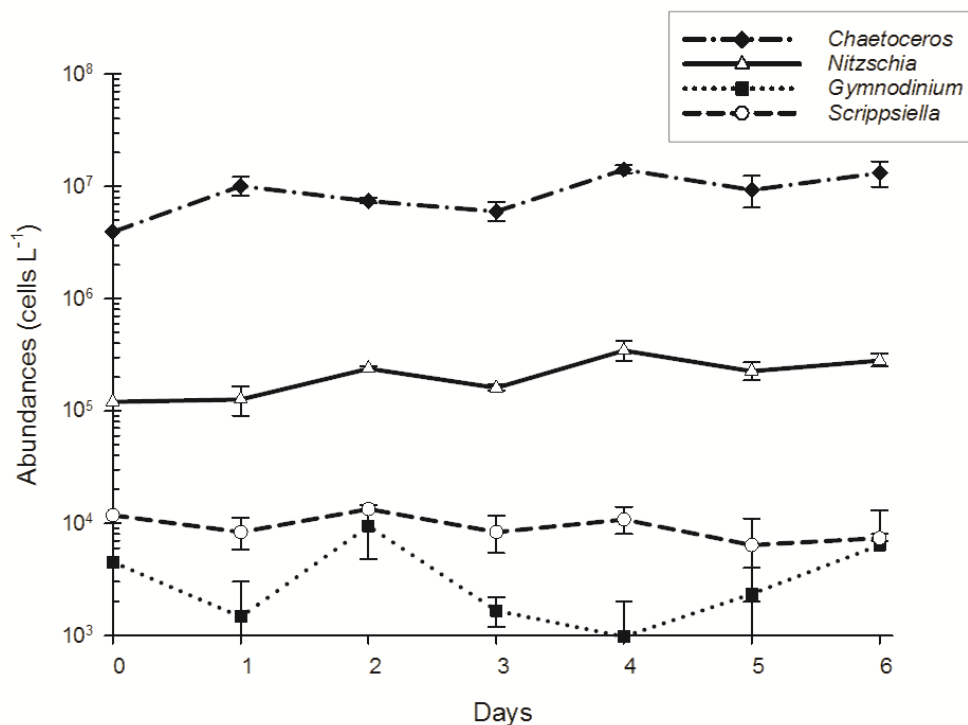


Figure 3.11: Mean cell abundances (cells L^{-1}) of *Chaetoceros sp.* (dash-dotted line with black diamonds), *Nitzschia sp.* (solid line with white triangle), *Gymnodinium sp.* (dotted line with black square) and *Scripsiella sp.* (dashed line with white circle) in the N-limited treatment. Error bars shown are standard errors (SE).

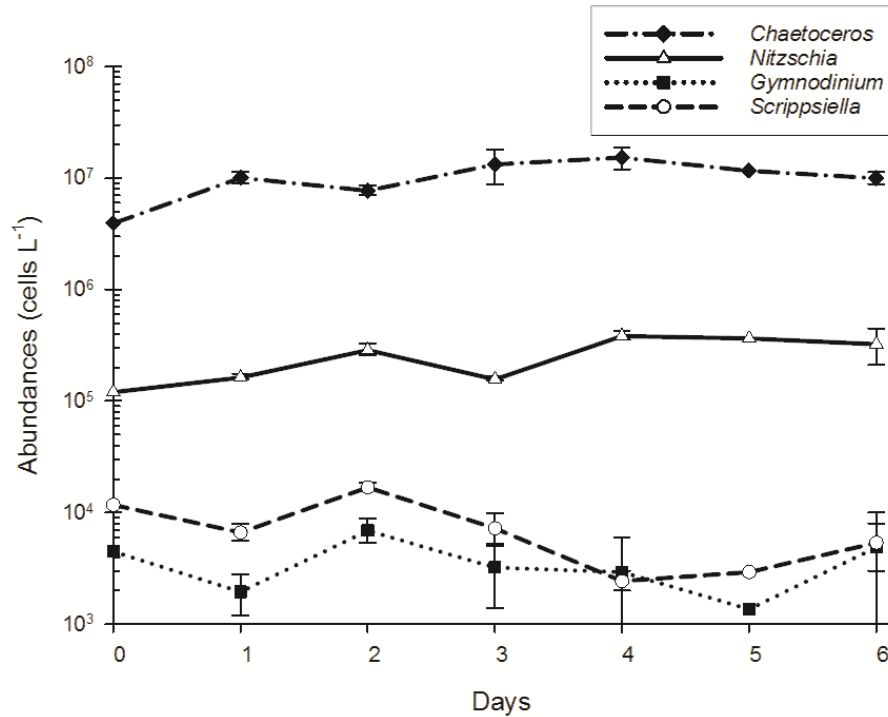


Figure 3.12: Mean cell abundances (cells L⁻¹) of *Chaetoceros* sp. (dash-dotted line with black diamonds), *Nitzschia* sp. (solid line with white triangle), *Gymnodinium* sp. (dotted line with black square) and *Scrippsiella* sp. (dashed line with white circle) in the P-limited treatment. Error bars shown are standard errors (SE).

Relatively high concentrations of chlorophyll *a* degradation products, *i.e.* pheide *a*, phe *a* and chl *a*, were found in Day 0 (Figures 3.13, 3.14 and 3.15). For instance, the (pheide *a* + phe *a*)/TChl *a*, an important pigment ratio that helps identify cell degradation (Roy et al., 2011), was ~19.8. Over the experiment, these pigments' concentrations had different developments: while pheophytin *a* (0.132 mg m⁻³) and chlorophyllide *a* (0.042 mg m⁻³) remained low, pheophorbide *a* average concentration was generally much higher (11.916 mg m⁻³; Table 2.3). In fact, pheophorbide *a* average concentration was over 40 times higher than the average total chlorophyll *a* (0.279 mg m⁻³). In the N-limited treatment, pheide *a* peaked on Day 2 (21.21 mg m⁻³), while in P-limited it only occurred on Day 3 (23.49 mg m⁻³). After peaking, pheide *a* decreased until the end of the experiment. On the Control treatment, however, pheide *a* concentrations had a declining trend, mirroring the chlorophyll *a* response.

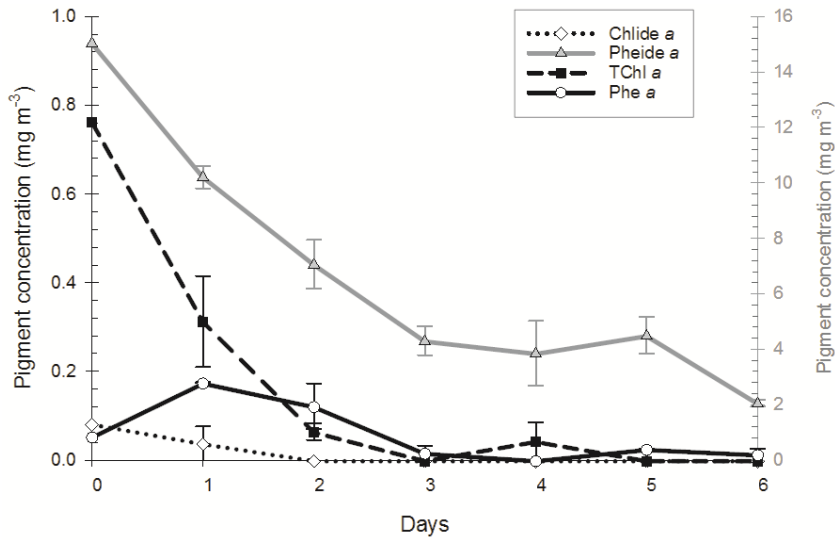


Figure 3.13: Total chlorophyll *a* (TChl *a*; dashed line with black squares) and chlorophyll *a* degradation products - chlorophyllide *a* (Chlide *a*; dotted line with white diamonds), pheophytin *a* (Phe *a*; solid line with white circles) and pheophorbide *a* (Pheide *a*; grey line with grey triangles) mean concentrations (mg m^{-3}) from Day 0 to Day 6 in the Control treatment. Error bars shown are standard errors (SE). Note that pheophorbide *a* concentrations are measured in the secondary axis (right, in gray).

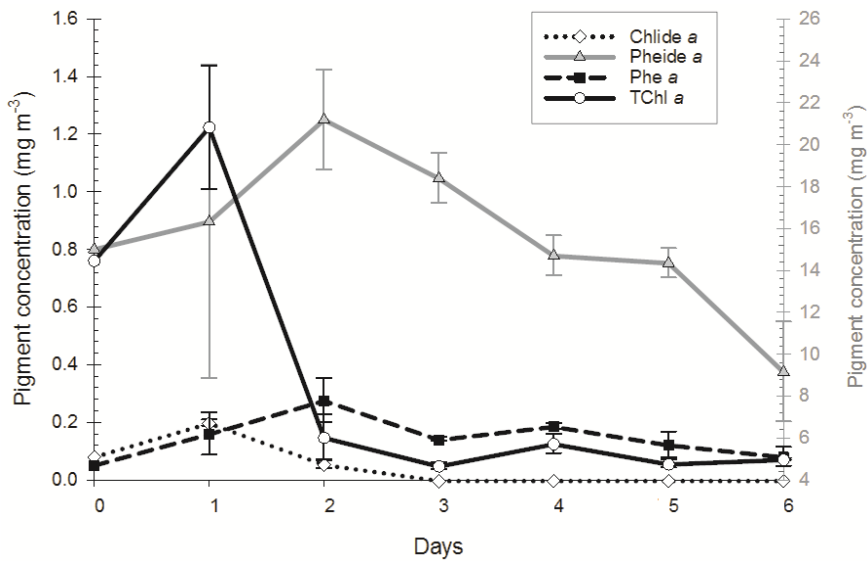


Figure 3.14: Total chlorophyll *a* (TChl *a*; dashed line with black squares) and chlorophyll *a* degradation products - chlorophyllide *a* (Chlide *a*; dotted line with white diamonds), pheophytin *a* (Phe *a*; solid line with white circles) and pheophorbide *a* (Pheide *a*; grey line with grey triangles) mean concentrations (mg m^{-3}) from Day 0 to Day 6 in the N-limited treatment. Error bars shown are standard errors (SE). Note that pheophorbide *a* concentrations are measured in the secondary axis (right, in gray).

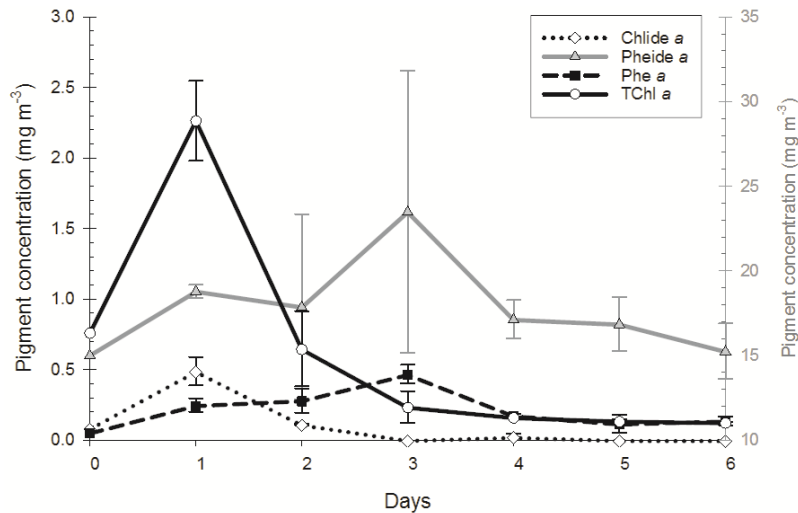


Figure 3.15: Total chlorophyll *a* (TChl *a*; dashed line with black squares) and chlorophyll *a* degradation products - chlorophyllide *a* (Chlide *a*; dotted line with white diamonds), pheophytin *a* (Phe *a*; solid line with white circles) and pheophorbide *a* (Pheide *a*; grey line with grey triangles) mean concentrations (mg m^{-3}) from Day 0 to Day 6 in the P-limited treatment. Error bars shown are standard errors (SE). Note that pheophorbide *a* concentrations are measured in the secondary axis (right, in gray).

Considering the accessory pigments detected by HPLC analysis (Table 2.3), chlorophyll *c*₂ (1.247 mg m^{-3}), fucoxanthin (0.331 mg m^{-3}) and MgDVP (0.139 mg m^{-3}) were the ones with the highest average concentrations. This suite of pigments is typical of red algal lineage groups like diatoms, which confirms cells abundance results. Like chl *a*, most accessory pigment concentrations seem to decrease after peaking in Day 1 except chlorophyll *c*₂ (Figures 3.16 and 3.17). In the N-limited treatment, chl *c*₂ concentrations peaked on Day 1 (2.26 mg m^{-3}) and decreased progressively until Day 6. In the P-limited treatment, it reached a maximum in Day 3 (2.91 mg m^{-3}) before slowly dropping to 1.37 mg m^{-3} . Apart from chl *c*₂, the variation of the other pigments was similar in both treatments. In general, pigments were found in higher concentrations in the P-limited treatment. Overall, the accessory pigments results suggest a general decrease in biomass during the experiment, contradicting the cell abundances results (Figure 3.7).

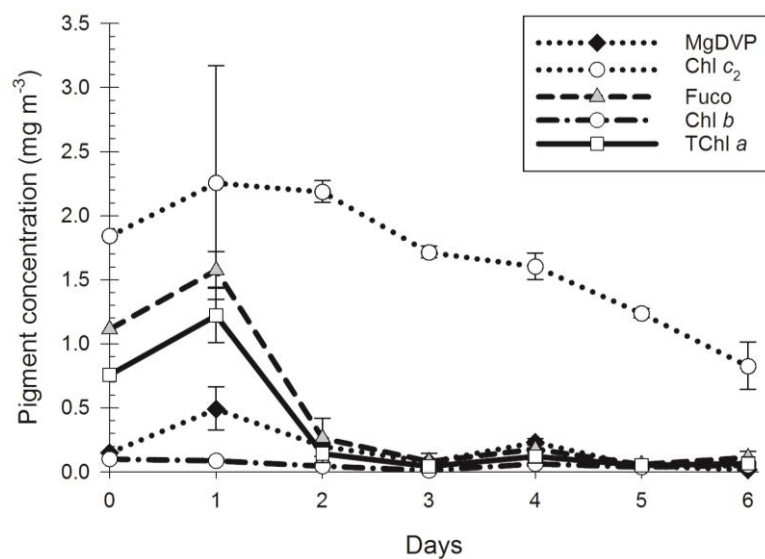


Figure 3.16: Mean concentrations (mg m^{-3}) of MgDVP (dotted line with black diamonds), chlorophyll *c*₂ (Chl *c*₂; dotted line with white circles), fucoxanthin (Fuco; dashed line with grey triangles), chlorophyll *b* (Chl *b*; dash-dotted line with white circles) and total chlorophyll *a* (TChl *a*; solid line with white squares) from Day 0 to Day 6 in the N-limited treatment. Error bars shown are standard errors (SE).

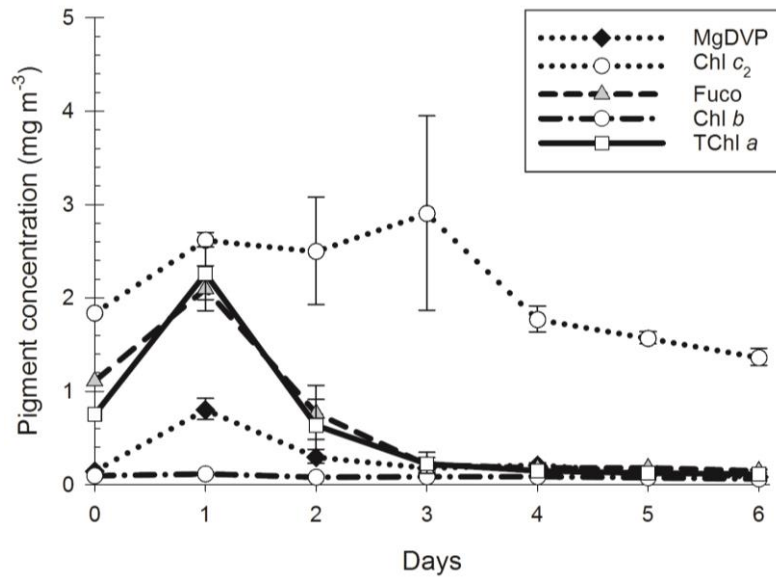


Figure 3.17: Mean concentrations (mg m^{-3}) of MgDVP (dotted line with black diamonds), chlorophyll c_2 (Chl c_2 ; dotted line with white circles), fucoxanthin (Fuco; dashed line with grey triangles), chlorophyll b (Chl b ; dash-dotted line with white circles) and total chlorophyll a (TChl a ; solid line with white squares) from Day 0 to Day 6 in the P-limited treatment. Error bars shown are standard errors (SE).

HPLC-CHEMTAX analysis revealed a diatom dominance of the phytoplankton community during the first days of the experiment, for both treatments (Figure 3.18 and 3.19). The peak in the absolute abundances of diatoms (0.65 mg m^{-3} in the N-limited treatment; 1.46 mg m^{-3} in the P-limited one) was achieved on Day 1. In the N-limited treatment, the diatom dominance seems to decrease as other phytoplankton groups like dinoflagellates, Chrysophyceae and Haptophyceae increase their relative contribution to total chlorophyll a . In the P-limited, the same decrease in diatoms were observed, however, it only occurred in Day 3. However, it is important to keep in mind that the absolute contributions to chl a are small ($<0.1 \text{ mg m}^{-3}$) since chlorophyll a concentrations are also low (see Figure 3.3).

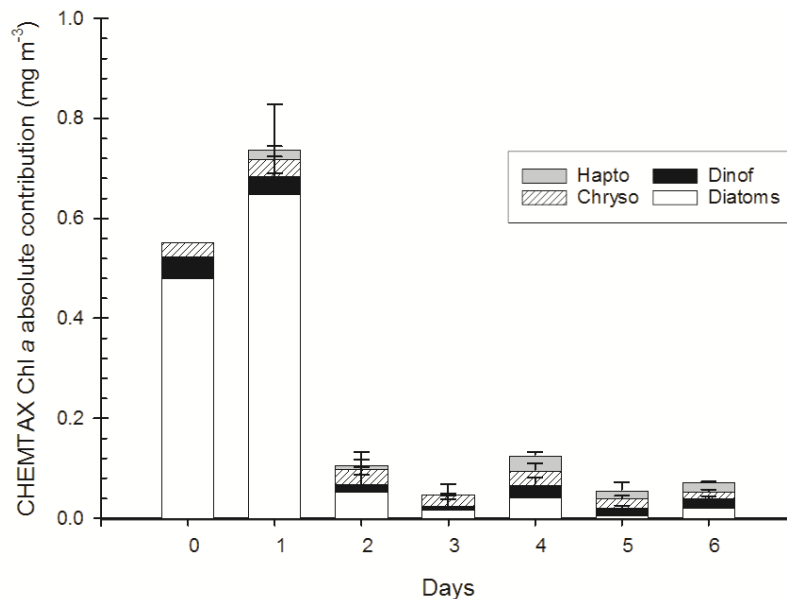


Figure 3.18: Chlorophyll a concentrations (absolute contribution; mg m^{-3}), estimated through the CHEMTAX analysis, for Haptophyceae (Hapto), dinoflagellates (Dinof), Chrysophyceae (Chryso) and diatoms from Day 0 to Day 6 in the N-limited treatment. Error bars shown are standard errors (SE).

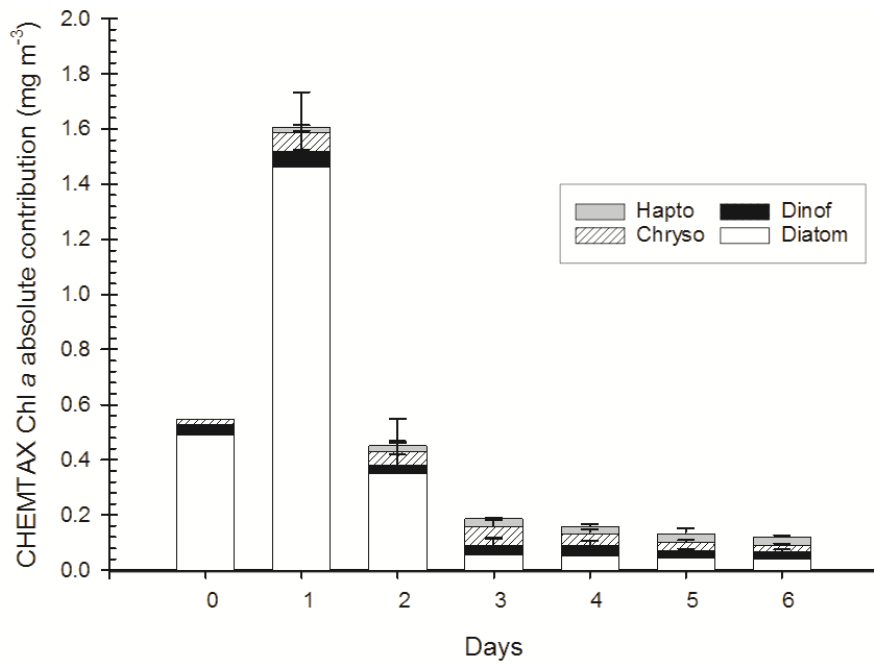


Figure 3.19: Chlorophyll *a* concentrations (absolute contribution; mg m⁻³), estimated through the CHEMTAX analysis, for Haptophyceae (Hapto), dinoflagellates (Dinof), Chrysophyceae (Chryso) and diatoms from Day 0 to Day 6 in the P-limited treatment. Error bars shown are standard errors (SE).

Considering data from both experimental treatments, there is no apparent relationship between cell numbers, obtained through microscopy, and pigment concentrations for diatoms (Figure 3.20; $R^2=0.05$) and dinoflagellates (Figure 3.21; $R^2=0.09$). However, when comparing only data regarding the first two days of the experiments, a good agreement between HPLC-CHEMTAX and cell counts was obtained ($R^2=0.71$; $p\text{-value}<0.05$; Figure 3.22). Dinoflagellates ($R^2=0.52$; $p\text{-value}<0.05$) were also in agreement, although the relationship observed was inverse (Figure 3.23).

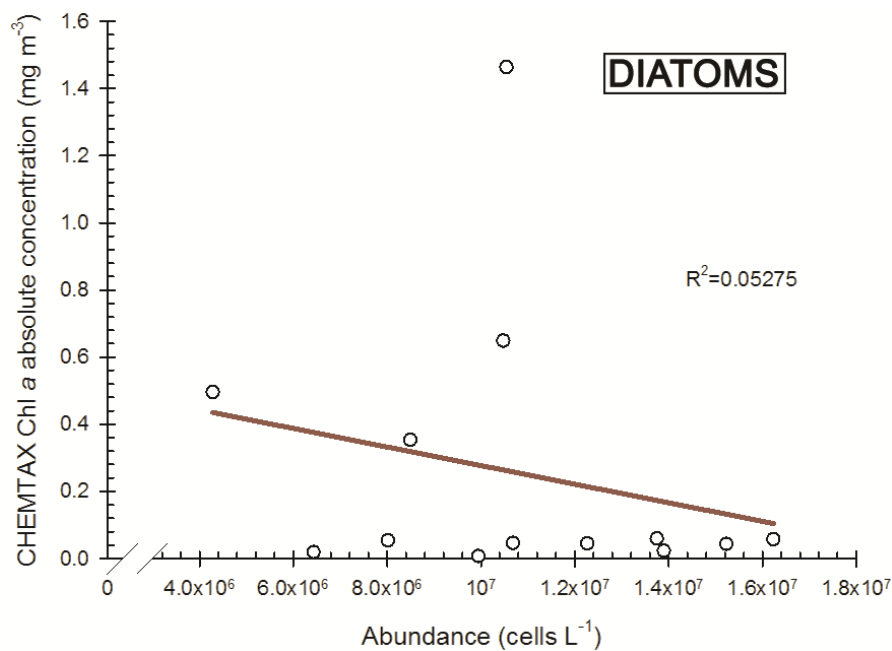


Figure 3.20: CHEMTAX chlorophyll *a* absolute concentrations (mg m⁻³) obtained through CHEMTAX for diatoms against diatoms abundances (cells L⁻¹) for both experimental treatments.

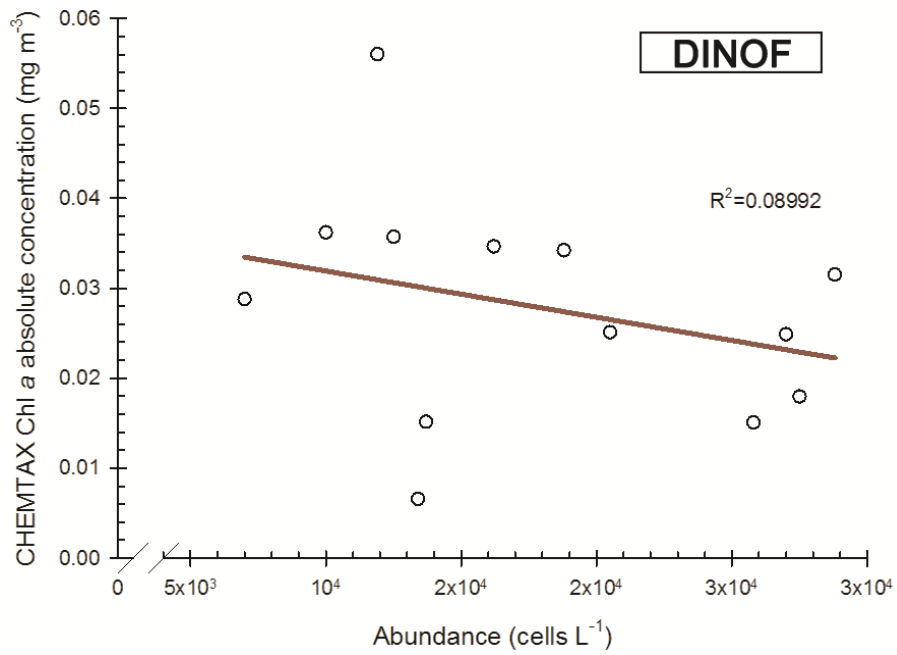


Figure 3.21: CHEMTAX chlorophyll *a* absolute concentrations (mg m^{-3}) obtained through CHEMTAX for dinoflagellates against dinoflagellates abundances (cells L^{-1}) for both experimental treatments.

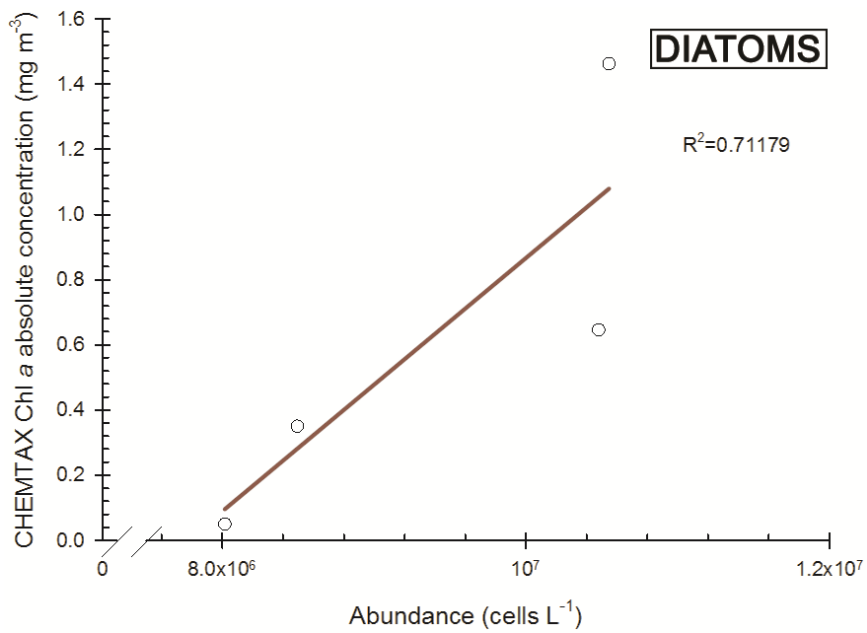


Figure 3.22: CHEMTAX chlorophyll *a* absolute concentrations (mg m^{-3}) obtained through CHEMTAX for diatoms against diatoms abundances (cells L^{-1}), only for Days 1 and 2, for both experimental treatments.

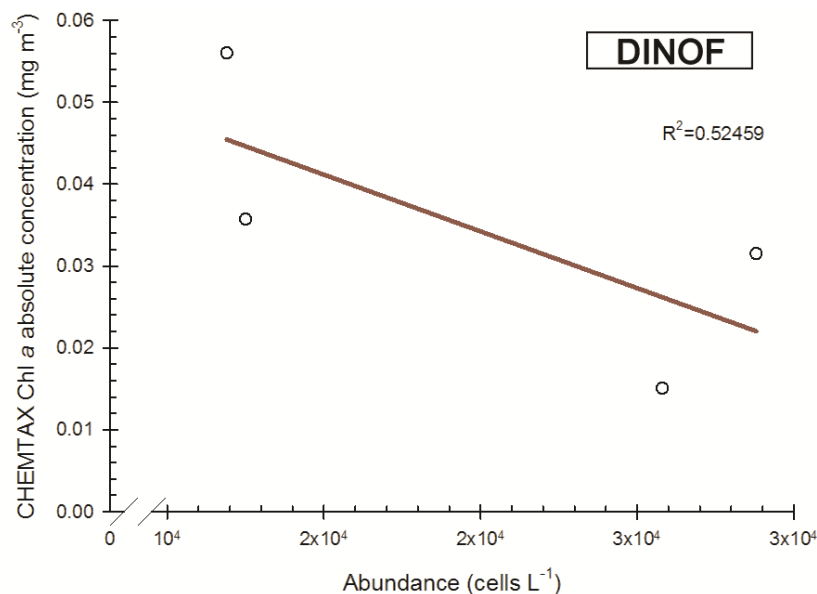


Figure 3.23: CHEMTAX chlorophyll *a* absolute concentrations (mg m^{-3}) obtained through CHEMTAX for dinoflagellates against dinoflagellates abundances (cells L^{-1}), only for Days 1 and 2, for both experimental treatments.

4. DISCUSSION

4.1. Post-bloom phytoplankton response to nutrient enrichment

Environmental conditions preceding the experiment suggest the existence of good conditions for upwelling and phytoplankton blooms in the weeks prior to water sampling. In fact, the concentrations of chlorophyll *a* degradation pigments (pheide *a* + phe *a*) were high compared to TChl *a*. The ratio (Pheide *a* + Phe *a*)/TChl *a* calculated for Day 0 (~19.8) indicated a post-bloom state of the phytoplankton community, particularly its high content in pheophorbide *a*, a chlorophyll *a* degradation product which is typically associated with grazing (Jeffrey, 1974; Roy, 1989; Schuman and Lorenzen, 1974; Vernet and Lorenzen, 1987). There is also a very low ratio of pheophytin-to-pheophorbide *a* (~0.004). Since pheophytin *a* is an intermediate product of pheophorbide *a* (Yentsch, 1967), this is a signal that chlorophyll *a* degradation could have occurred for some time (Schuman and Lorenzen, 1974).

The results of the experiment show that there is a clear response from the phytoplankton community to the first pulse of enrichment, regardless of which treatment the microcosms were subject to. Both chlorophyll *a* concentration and cell abundance peaked in the following day to the initial enrichment pulse (Figures 3.3 and 3.7), suggesting the phytoplankton community's main response to an enrichment pulse occurred in the first day prior to the pulse. Comparing with a similar experiment conducted by Edwards et al. (2005) in southern Portugal, where chlorophyll *a* only peaked ($26.5 \mu\text{g L}^{-1}$ in Ria Formosa and $70.6 \mu\text{g L}^{-1}$ in Sagres) after 4/5 days, this seems to be a fast response. Almost 40 years prior to this study, Thomas et al. (1974) experimented with phytoplankton samples from a coastal region near southern California and determined that phytoplankton, in general, peaked two days after the enrichment began. It also concluded that diatoms' response to the enrichment was faster than what was observed for dinoflagellates. Despite having low surface to volume ratios, thus not being as efficient as other taxa in oligotrophic conditions (Chisholm, 1992; Reynolds, 2006), diatoms, in general, have characteristics which enables faster growth when sufficient nutrients are available (Furnas, 1990) such as high nutrient uptakes rates (Lomas and Gilbert, 2000), high half-saturation constants (Eppley et al., 1969) and high resistance against viruses (Sarhou et al., 2005).

Furthermore, some larger diatoms can migrate vertically to waters below the nutricline, where nutrients are in higher concentrations (e.g. McKay et al., 2000). Other strategies like the storage of surplus nutrient concentration in vacuoles (e.g. Eppley and Coatsworth, 1968) show that diatoms are clearly well adapted to dynamic waters and rapid changes in nutrient availability. Thus, not only the local environmental conditions influence how fast phytoplankton respond to an enrichment pulse, but also its composition. This could help explain the short response time identified in the present study, since the water samples were collected from a coastal region and its phytoplankton community was mainly composed of diatoms. The fast response of the post-bloom community could also have been caused by the consumption of luxurious nutrients by the phytoplankton during the days that preceded the experiment. However, the fact that this phytoplankton community generally lives under recurring upwelling conditions could also have had an influence. Since recurrent upwelling events act as nutrient enrichment pulses, the community could be adapted to these nutrient inputs and grow faster when such events occur.

Until peaking, the communities of both experimental treatments had identical cell abundance responses to the enrichment. Yet, after the decline in Day 2, cell abundances in the P-limited treatment increased once more (Figure 3.7), opposing the decline observed in the N-limited treatment samples. Such difference might have been associated with the concentration of DIN available by Day 2 (Figure 3.4). Although nutrient demand varies with cell size, shape and composition, a phytoplankton cell with 20 μm diameter, assuming spherical geometry and diffusive transport only (i.e. excluding, for example, active transport, a major part of cellular nutrient transport) requires, at least, 1.3 μM of DIN to meet its demand in DIN and grow at a maximum rate of 1 d^{-1} (Williams et al., 2002). As a comparison, a typical cell of *Chaetoceros debilis*, one of the most abundant *Chaetoceros* species in coastal Chile, can have a large diameter (apical axis) of 8-40 μm (Hasle and Syvertsen, 1997). However, this value can be influenced by the nitrogen compound. Ammonium (NH_4^+) utilization requires less metabolic energy (Guerrero et al., 1981). Thus, its uptake was assumed to be favoured by phytoplankton in comparison with other DIN compounds, such as nitrate or nitrite (Dortch, 1990; Dugdale et al., 2007). However, some studies have reported that diatoms seem to favour the assimilation of nitrate (Lomas and Glibert, 1999a, 1999b). Consequently, the fact that the community was mainly composed by diatoms and that nitrate was chosen as the nitrogen source in the experimental enrichments could have had a major impact in diatoms' growth.

Since DIN concentration in the N-limited treatment was approximately zero in Day 2 (Figure 3.4), this could have been insufficient for the growth of larger phytoplankton like diatoms, even when considering luxury consumption from internal vacuoles. On the other hand, the P-limited treatment microcosms still had enough DIN (3.2 μM), which could have been enough for the phytoplankton community to bounce back.

Altogether, the main group to benefit from the enrichment pulse were diatoms, mainly centric diatoms. Their increase in biomass by over two-fold established centric diatoms as the dominant group in the community. On the other hand, phytoflagellates and dinoflagellates' cell numbers decreased. Similar transitions to diatom dominance after enrichment events have been documented (Edwards et al., 2005; Parsons et al., 1978). In Edwards et al. (2005) enrichment experiments, two distinct communities with initially low diatom abundance transitioned to a community mainly composed of diatoms only a few days after the enrichment pulse. Even in situations where diatoms originally dominated the community, they tended to remain dominant or at least the most abundant group (D'Elia et al., 1986; Sanders et al., 1987; Stockner and Shortreed, 1978; Sundbäck and Snoeijs, 1991). In addition, nitrate is known to be the main DIN compound in upwelling-derived nutrient inputs (Capone and Hutchins, 2013). Since, as mentioned above, nitrate was used and diatoms favour its assimilation (Lomas and Glibert, 1999a, 1999b), this could have contributed to this situation. Moreover, the lack of grazers in the microcosms must also have contributed to the increase of diatoms.

As for phytoflagellates and dinoflagellates' losses, competitive exclusion (Hardin, 1960), *i.e.*, the sequester of the available nutrients by diatoms, probably in excess due to luxury uptake, could have limited their growth.

However, any of these factors could not have been sufficient for causing the cell losses verified. Thus, these losses might be related with the initial post-bloom situation, as a substantial percentage of the cells could have already been under degradation and decline in Day 0. In such case, these cells would have collapsed, counterbalancing whatever population growth could have been promoted by the nutrient enrichment. Moreover, the possibility of predation from small grazers that could have passed through by the 200 μm mesh should not be disregarded as well.

Although *Chaetoceros sp.* was the most abundant diatom taxon by a large margin, other diatom taxa like *Nitzschia sp.* or *Skeletonema sp.* were also plentiful. These taxa are common in regions affected by coastal upwelling events (*e.g.* Estrada & Blasco, 1985; Lassiter et al., 2006) and have been observed in areas nearby, such as the coastal area off Concépcion (~36.5°S; Anabalón et al., 2007; González et al., 2007; 1987). The dominance of *Chaetoceros sp.* will be approached in a more detailed manner in section 4.3. Most of the phytoflagellates' cells identified belonged to Chrysophyceae and Cryptophyceae. These results are interesting, since both these groups have been detected at their lowest abundances during upwelling season (*e.g.* Glenn et al., 2004; Goela et al., 2014). Dinoflagellates were only found in small abundances, which was expected since their growth typically favours low turbulence (Margalef, 1978).

4.2. Phytoplankton response to nutrient enrichment: Additional pulses

While phytoplankton response to an enrichment pulse can lead to an increase in biomass, its reaction to an additional pulse might be different as it could be influenced by the community's response to the original pulse. In these experiments, at least for cell abundances data, the impact of the additional enrichment pulse appears to be additive as it led to higher abundances than the previous pulse (Figure 3.7). Chlorophyll *a* data, on the other hand, showed only minor to no influence on the community's biomass (Figure 3.3; more on section 4.4). However, it should be noted that if the second enrichment pulse had occurred earlier or later than the established, the result might have been different. While there was a biomass increase in both treatments, the impact was more noticeable in the N-limited treatment. This difference is most likely related with the absence of available DIN in the N-limited microcosms in Day 3 (Figure 3.4). The input of nitrate, thus, must have jumpstarted the community.

After peaking, cell abundances decreased slightly in Day 5. This behaviour mirrored the decline seen in the first half of the experiment, when cell numbers dropped in both treatments after peaking (Day 2). This decline continued in the P-limited samples, but not in the N-limited ones. However, due to the high variability associated with Day 6 abundances values, it is not reasonable to make conclusions. In general, the phytoplankton decline in both treatments is clearly more gradual than what was observed after the initial enrichment pulse. Thus, the cause of this decline is probably different than the decline seen after the first enrichment. Since phytoplankton still had sufficient available nutrients to grow, particularly in the P-limited treatment (Figures 3.4 and 3.5), there could have been limitation in other micronutrients. Phytoplankton iron (Fe) limitation, for example, has been reported by several studies in the Humboldt Current System (*e.g.* Bruland et al., 2005; Hutchins et al., 2002; Torres and Ampuero, 2009). Fe limitation in upwelling regions is usually provoked by the combination of major nutrients (*e.g.* N or P) inputs from upwelling and low Fe inputs from rivers and continental shelf sediments (Hutchins et al., 2002). Since river runoff in northern-central Chile is of minor importance (Thiel et al., 2007), it is possible that, after the pre-experiment bloom and the recurrent growth observed during the experiment period, the community underwent Fe limitation.

Considering the phytoplankton community's composition, the impact of the additional pulse was not as extreme as the initial pulse. In fact, all major phytoplankton groups abundances increased in the N-limited treatment and while phytoflagellates do replace pennate diatoms as the second most abundant group, their cell abundances are similar (Figure 3.9). In the P-limited treatment, despite a decrease in dinoflagellates, the situation is mostly alike since centric diatoms continue to dominate the communities (Figure 3.10). This suggests additional enrichment pulses of the same nature might not have a major impact in the community composition despite clearly increasing total cell abundances. This, however, may change with the frequency of the enrichments pulses. For example, in Gaedeke & Sommer's experience (1986), enrichment pulses administered daily to the mesocosms increased the dominance of the most abundant species, leading to a very low diversity community after a few days. Nonetheless, these experiments were done with freshwater phytoplankton and may not reflect what happens in an upwelling affected region. This is a subject where knowledge is scarce, since research is mainly focused on the phytoplankton community's behaviour after or during single upwelling event. Such knowledge gap would be worth exploring since recent studies suggest a potential increase in the intensity and duration of upwelling events in some of the major eastern boundary upwelling systems, including the Humboldt one (Wang et al., 2015).

Overall, the studied phytoplankton community reacted similarly when subjected to nutrient enrichment pulses, whether these pulses imposed a change in the limited nutrient or not. The only difference appeared to be a slightly larger percentage of Chrysophyceae and Cryptophyceae in the samples subjected to the N-limited treatment. Other than that, the abundances values were similar for both treatments. This contradicted initial expectations since, as marine coastal phytoplankton is typically limited in nitrogen, it was predicted that phytoplankton biomass would be higher in the P-limited treatment after the enrichment pulses. Nevertheless, chlorophyll *a* data did show a significantly higher response to the first pulse in the P-limited treatment (Figure 3.3). This discrepancy could indicate that smaller phytoplankton, easily neglected during light microscopy, might have responded differently to the imposed nutrient limitations.

The similar behaviour observed in both treatments might be explained by the nitrate-to-phosphate ratios (Figure 3.6). Even though the enrichments pulses in the P-limited were designed to implement phosphorus-limited conditions, the N:P ratio had a downward trend to values under, indicating N-limitation. This confirms the community is clearly adapted to nitrogen limitation, since it consumes the available nitrogen at a much higher rate than it consumes phosphorus. Thus, it can be argued that a phytoplankton community living in N-limited waters does not easily adapt to phosphorus limitation, even when such conditions are imposed as a result of an enrichment pulse. Throughout this experiment, and with two enrichment pulses in between, the community still remained intrinsically limited by nitrogen. However, the N:P ratio decline after the second enrichment pulse was less steep, a consequence of the possible Fe limitation seen during the second half of the experiment.

4.3. *Chaetoceros* dominance

Since *Chaetoceros* sp. highly dominated the community by composing over 90% of total cell abundances, it is essential to address why this happened. *Chaetoceros* is highly abundant in the Chilean coast and, along with *Skeletonema* and *Thalassiosira*, is one of the key diatom genera associated with coastal upwelling (Koch & Rivera, 1984; Romero & Hebbeln, 2001; 2003). This is supported by the predominance of *Chaetoceros* spp. spores in the diatom thanatocoenosis along the coast (Romero and Hebbeln, 2003), particularly between 30°S-38°S, which includes Algarrobo Bay (~33°S). Furthermore, *Chaetoceros* spp. is particularly abundant in other upwelling associated regions during the upwelling season (e.g. Abrantes and Moita, 1999; Hutchins et al., 1998; Pitcher, 1990), thus explaining *Chaetoceros* presence as one of the main taxa identified in this study.

Diatoms are known to bloom in coastal areas where there has been a recent anthropogenic or natural nutrient input, as long as there is enough silicon (Bruland et al., 2005; De Baar et al., 1995). Interestingly, the control treatment in the present study also displays diatom dominance, particularly after Day 0 (Figure 3.8). This means that, while the nutrient inputs stimulated diatom growth in the experimental treatments, they were not responsible for their dominance during the experiment.

To understand phytoplankton's response under different environmental conditions, one has to consider their life strategy: C, R or S (see Reynolds, 1988, 1996 for more detailed information), for instance. These strategies take into account the cells' MLD (maximum linear dimension) and S/V (surface-to-volume) ratio (Reynolds, 1996) and have been used extensively in the last 20 years (e.g. Alves-de-Souza et al., 2006, 2008; Huszar and Caraco, 1998; Padisák and Reynolds, 1998; Smayda & Reynolds, 2001, 2003). *Chaetoceros* spp. are usually considered as R-strategists – organisms with relatively high S/V ratio ($\sim 1 \mu\text{m}^{-1}$), which grow preferentially under nutrient-rich turbulent conditions (Reynolds, 1984) – although several studies have noted that some of its species are abundant under low turbulence and can also be considered as C-strategists (e.g. Bonilla et al., 2005; Brito et al., 2015). This is not the case in the present study as *Chaetoceros* sp. growth and dominance in enriched and turbulent microcosms are a clear sign of its role as an R-strategist. In 2008, Alves-de-Souza et al. focused on the marine diatom communities of the Chilean fjords and identified 3 distinct groups: D1, D2 and D3 (see Alves-de-Souza et al. 2008). In this study, several *Chaetoceros* species made up group D2: species with S/V circa $1 \mu\text{m}^{-1}$ and associated with turbulence and nitrate. The large abundances of *Chaetoceros* sp. found in the current study support these findings and shed some light on how different life strategies can influence the growth of diatoms in an upwelling succession.

Thus, *Chaetoceros* sp. dominance is most probably related to two reasons: i) large chain-forming diatoms like *Chaetoceros* sp. have high nitrate uptake rates, giving them a major competitive edge in rapidly consuming the available nitrogen (Fawcett and Ward, 2011; Van Oostende et al., 2015) and establishing them as D2 diatoms, ii) the absence of large grazers in the microcosms, which are typically responsible for the short duration of *Chaetoceros* spp. blooms (Van Oostende et al., 2015). Some *Chaetoceros* species are considered as harmful, having already caused a variety of fish mortality events (e.g. Hellenen, 2016; Yang and Albright, 1992). These species have setae, long protective siliceous spines with, which can break during the fish's feeding and penetrate its gill membranes. As a result, mucus, in excess, is produced and inhibits oxygen diffusion, leading to death by suffocation (Yang and Albright, 1992). Bell et al. (1974) showed that concentrations of, at least, 5×10^3 cells L^{-1} can be lethal for salmonids. Thus, if grazing is inefficient, *Chaetoceros* sp. can be a nuisance in certain cases. Further studies on the relationship between *Chaetoceros* sp. and its grazers could lead to valuable information for managing such cases.

4.4. Changes in pigment and photoacclimation

Pigment analysis is regarded as a useful complementary approach to cell counts in phytoplankton ecology studies, particularly regarding smaller taxa which could be when counting and identifying the cells (Brito et al., 2015; Schlüter et al., 2000). However, it has its limitations and depending solely on pigment data might lead to misleading conclusions (Irigoién et al., 2004). The current study is a good example of its limitations. Pigment average concentrations (Table 2.3) suggest a community mainly made up by phytoplankton groups belonging to the red algal lineage, which is in agreement with the high abundances of diatoms (Table 3.1). However, pigment data for most of the experiment period contradicts cell counts. This contradiction is verified after Day 1 as pigment concentrations drop throughout the experiment while cell abundances rise.

Such incongruence reflected on the HPLC-CHEMTAX analysis, leading to very different results than the obtained through cell counts. For example, the phytoplankton community at Day 6 in

the N-limited treatment was identified as a community with nearly equal proportions of diatoms, dinoflagellates, Chrysophyceae and Haptophyceae (Figure 3.18). Cell counts, on the other hand, reveal a community ~98% made of diatoms (Figure 3.9). Comparing HPLC-CHEMTAX and cell counts results for the first two days appears to support the idea that this contradiction only occurred after Day 1, at least for diatoms (Figures 3.20 and 3.22). If the decrease in chlorophyll *a* and other photosynthetic pigment concentrations were a consequence of cell losses, there would have been a substantial overall increase in chlorophyll *a* degradation products. While there is indeed an increase in pheophorbide *a* (pheide *a*) in the N-limited treatment after Day 1 (Figure 3.14), this increase does not appear to be enough to justify the steep drop in chl *a*. Moreover, in the P-limited treatment, pheide *a* concentration did not increase as chl *a* dropped in Day 2 (Figure 3.15). Furthermore, in the Control treatment, pheide *a* displayed an overall decrease, accompanying the decline of chlorophyll *a* (Figure 3.13). Thus, there must have been another reason for the sharp decline observed for the photosynthetic pigments. Since the environmental conditions remained stable during the experiment, it can be hypothesized that these also did not trigger the decline in pigments concentrations. Therefore, it is possible that the observed decline was a consequence of photoacclimation by the phytoplankton community.

Photoacclimation is a short-term phenomenon characterised by the adjustment of the photosynthetic machinery in phytoplankton cells as a reaction to a severe change in light conditions (Dubinsky and Stambler, 2009). When phytoplankton is subject to a new environment where the light conditions are very high, they typically lower the amount of photosynthetic pigments, while increasing the amount of photoprotective ones, such as photoprotective carotenoids (PPC; Rodriguez et al., 2009). This allows phytoplankton to endure and grow while avoiding photodynamic damage (Stambler and Dubinsky, 2007).

In its natural environment, some phytoplankton, such as several phytoflagellates, may migrate vertically to protect their photosynthetic apparatus from damage caused by ongoing high light incidence. In this study, since the microcosms were stored on the exterior, they were subject to natural sunlight. Although they were protected from direct sunlight to avoid such problems, this may not have been enough, leading to photoacclimation. Since there was a general decline in pigment concentration from Day 1 to Day 2, photoacclimation must have occurred between that period, although it could have started earlier and only been noticed in that period. Previous experiments suggest photoacclimation to dark environments takes longer than photoacclimation to bright environments because the increase in pigment content has to compensate for its dilution due to cell division (Post et al., 1984; Prézelin et al., 1991). In environments with high nutrient availability, photoacclimation to high-light conditions may range from hours to days (e.g. Cullen and Lewis, 1988; Post et al., 1984; Prézelin and Matlick, 1983; Rivkin et al., 1982; Sukenik et al., 1990). In Post et al. (1984) experiments with *Thalassiosira weissflogii*, photoacclimation started a few hours after the light intensity change and lasted roughly 30h until the cell's content in chl *a* stabilized at much lower values. These values are comparable with the ones found in the present study. However, most of these studies focused on sudden changes from low to high light conditions or vice versa, which may not have been the case.

Depth related problems like this may happen in phytoplankton experiments (Dudzik et al., 1979), which stresses the importance of also relying in other complementary techniques like cell counts. The solar protection should be increased in future experiments to avoid photoacclimation. Another possible solution would be to increase the frequency of agitation of the microcosms, which would help maintain high turbulence. This could reduce light availability along the microcosm, thus contributing to avoid photoacclimation.

4.5. Final considerations

Nutrient-enrichment experiments such as the ones conducted in this study are crucial for understanding how phytoplankton growth and composition relates to nutrients (Domingues et al., 2015). They provide invaluable information that can be used as a management tool, for instance, in cases where it is necessary to assess the impact of a nutrient discharge (Gobler et al., 2006). As coastal systems become increasingly under pressure and nutrient discharges in marine waters, such as from untreated urban waste waters, worsen, the need for these studies has never been as high.

There are several results that are relevant to further understand how phytoplankton communities respond to nutrient enrichment events, as well as contribute to water management strategies: i) phytoplankton in typically upwelling regions appears to have fast responses to sudden changes in nutrient availability; ii) while biomass was slightly higher under phosphorus-limitation, the community's composition was very similar in both treatments; iii) after the second enrichment pulse, micronutrient limitation, possibly in iron, might have constrained phytoplankton growth, highlighting the role of iron as key micronutrient in this region and iv) the dominance of diatoms, especially *Chaetoceros* sp., stresses their growth advantages to other groups and underlines the importance of grazers for the control of microphytoplankton in these regions.

This information is relevant for understanding the functioning of phytoplankton communities and its effects to the whole ecosystem dynamics. A good understanding on how phytoplankton responds to a stimulus can provide insights into its possible implications to the food webs. Therefore, such information is essential for environmental quality assessment and resource management in aquatic habitats. Furthermore, it can also be used for managing nutrient loads-related problems in the Chilean coastal zone and be extrapolated for similar oceanographic areas in the Chilean coast and, more importantly, to other Upwelling Systems throughout the world. Despite their differences in nutrient availability, primary productivity and upwelling strength and timings, all upwelling systems have a common predominance of diatoms and similar nitrogen limitation conditions during upwelling season. Thus, the responses of the phytoplankton community considered in this study may be similar to those observed in these regions, particularly in the ones where Fe limitation can occur, such as the California coastal upwelling system.

REFERENCES

- Abrantes, F., Moita, M.T., 1999. Water column and recent sediment data on diatoms and coccolithophorids, off Portugal, confirm sediment record of upwelling events. *Oceanol. Acta*, 22, 319-336.
- Alves-de-Souza, C., Menezes, M., Huszar, V., 2006. Phytoplankton composition and functional groups in a tropical humid coastal lagoon, Brazil. *Acta Bot. Bras.* 20, 701-708.
- Alves-de-Souza, C., González, M.T., Iriarte, J.L., 2008. Functional groups in marine phytoplankton assemblages dominated by diatoms in fjords of southern Chile. *J. Plankton Res.* 30, 1233-1243.
- Ansari, A.A., Gill, S.S., Lanza, G.R., Rast, W., 2011. *Eutrophication: causes, consequences and control*. Springer, Dordrecht.
- Anabalón, V., Morales, C.E., Escribano, R., Varas, M.A., 2007. The contribution of nano- and microplanktonic assemblages in the surface layer (0-30m) under different hydrographic conditions in the upwelling area off Concepción, central Chile. *Prog. Oceanogr.* 75, 396-414.

- Atlas, E.L., Hager, S.W., Gordon, L.I., Park, P.K., 1971. A practical manual for use of the Technicon AutoAnalyzer in seawater nutrient analyses; revised. Technical Report, vol. 215. Oregon State University, Corvallis.
- Bell, G.R., Griffioen, W., Kennedy, O., 1974. Mortalities of pen-reared salmon associated with blooms of marine algae. P. Northwest Fish Cult. Conf., Seattle, WA. 153 pp.
- Bonilla, S., Conde, D., Aubriot, L., Pérez, M. del C., 2005. Influence of hydrology on phytoplankton species composition and life strategies in a subtropical coastal lagoon periodically connected with the Atlantic Ocean. *Estuaries*, 28, 884-895.
- Brzezinski, 1985. The Si:C:N ratio of marine diatoms: interspecific variability and the effect of some environmental variables. *J. Phycol.* 21:347-357.
- Brito, A.C., 2010. The development of an assimilative capacity model for the sustainable management of nutrients within the Ria Formosa in southern Portugal. PhD thesis. Edinburgh Napier University.
- Brito, A.C., Newton, A., Tett, P., Icely, J., Fernandes, T.F., 2010. The yield of microphytobenthic chlorophyll from nutrients: Enriched experiments in microcosms. *J. Exp. Mar. Bio. Ecol.* 384, 30-43.
- Brito, A.C., Sá, C., Mendes, C.R., Brand, T., Dias, A.M., Brotas, V., Davidson, K., 2015. Structure of late summer phytoplankton community in the Firth of Lorn (Scotland) using microscopy and HPLC-CHEMTAX. *Estuar. Coast. Shelf S.* 167, 86-101.
- Bruland, K.W., Rue, E.L., Smith, G.J., DiTullio, G.R., 2005. Iron, macronutrients and diatom blooms in the Peru upwelling regime: brown and blue waters of Peru. *Mar. Chem.* 93, 81-103.
- Cabrita, M.T., Silva, A., Oliveira, P.B., Angélico, M.M., Nogueira, M., 2015. Assessing eutrophication in the Portuguese continental exclusive economic zone within the European Marine Strategy Framework Directive. *Ecol. Indic.*, 58, 286-299.
- Capone, D.G., Hutchins, D.A., 2013. Microbial biogeochemistry of coastal upwelling regimes in a changing ocean. *Nat. Geosci.* 6, 711-717
- Carpenter, S.R., 1996. Microcosm experiments have limited relevance for community and ecosystem ecology. *Ecology* 77, 677-680.
- Carpenter, S.R., Caraco, N.F., Correll, D.L., Howard, R.W., Sharpley, A.N., Smith, V.H. 1998. Nonpoint pollution of surface waters with phosphorus and nitrogen. *Ecol. Appl.* 8:559-568.
- Carr, M.E., 2002. Estimation of potential productivity in eastern boundary currents using remote sensing. *Deep-Sea Res. Pt. II.* 49:59-80.
- Chavez, F.P., Messié, M., 2009. A comparison of eastern boundary upwelling ecosystems. *Prog. Oceanogr.* 83:80-96.
- Chavez, F.P., Bertrand, A., Guevara-Carrasco, R., Soler, P., Csirke, J., 2008. The Northern Humboldt current system: brief history, present status and a view towards the future. *Prog. Oceanogr.* 79, 95-105.

- Chrétiennot-Dinet, M., 1990. Atlas du Phytoplancton Marin. III. Chlorarachniophycées, Chlorophycées, Chrysophycées, Cryptophycées, Euglénophycées, Eustigmatophycées, Prasinophycées, Prymnesiophycées, Rhodophycées et tribophycées. Centre National de la Recherche Scientifique, Paris. France.
- Cullen, J.J., Lewis, M.R., 1988. The kinetics of algal photoadaptation in the context of vertical mixing. *J. Plankton. Res.* 10, 1039-1063.
- Cury, P.M., Shin, Y.J., Planque, B., Durant, J.M., Fromentin, J.M., Kramer-Schadt, S., Stenseth, N.C., Travers, M., Grimm, V., 2008. Ecosystem oceanography for global change in fisheries. *Trends Ecol. Evol.* 23:338-346.
- D'Elia, C.F., Sanders, J.G., Boynton, W.R., 1986. Nutrient enrichment studies in a coastal plain estuary: phytoplankton growth in large-scale, continuous cultures. *Can. J. Fish. Aquat. Sci.* 43, 397-406.
- De Baar, H.J.W., de Jong, J.T.M., Bakker, D.C.E., Löscher, B.M., Veth, C., Bathmann, U., Smetacek, V., 1995. Importance of iron for plankton blooms and carbon dioxide drawdown in the Southern Ocean. *Nature*, 373, 412-215.
- Domingues, R.B., Guerra, C.C., Barbosa, A.B., Galvão, H.M., 2015. Are nutrients and light limiting summer phytoplankton in a temperate coastal lagoon? *Aquat. Ecol.* 49, 127-146.
- Dortch, Q., 1990. The interaction between ammonium and nitrate uptake in phytoplankton. *Mar. Ecol. Prog. Ser.* 61, 183-201.
- Dubinsky, Z., Stambler, N., 2009. Photoacclimation processes in phytoplankton: mechanisms, consequences, and applications. *Aquat. Microb. Ecol.*, 56, 163-176.
- Dudzik, M., Harte, J., Jassby, A., Lapan, E., Levy, D., Rees, J., 1979. Some considerations in the design of aquatic microcosms for plankton studies. *Int. J. Environ. Stud.* 13, 125-130.
- Dugdale, R.C., Wilkerson, F.P., Hogue, V.E., Marchi, A., 2007. The role of ammonium and nitrate in spring bloom development in San Francisco Bay. *Estuar. Coast. Shelf. S.* 73, 17-29.
- Edwards, V., 2001. The Yield of Marine Phytoplankton Chlorophyll from Dissolved Inorganic Nitrogen under Eutrophic Conditions. PhD Thesis. Edinburgh Napier University.
- Edwards, V.R., Tett, P., Jones, K.J., 2003. Changes in the yield of chlorophyll *a* from dissolved available inorganic nitrogen after an enrichment event — applications for predicting eutrophication in coastal waters. *Cont. Shelf Res.* 23, 1771–1785.
- Edwards, V., Icely, J., Newton, A., Webster, R., 2005. The yield of chlorophyll from nitrogen: A comparison between the shallow Ria Formosa lagoon and the deep oceanic conditions at Sagres along the southern coast of Portugal. *Estuar. Coast. Shelf Sci.* 62, 391–403.
- Eppley, R.W., Coatsworth, J.L., 1968. Uptake of nitrate and nitrite by *Ditylum brightwelli* — kinetics and mechanisms. *J. Phycol.* 4, 151-156.
- Eppley, R.W., Rogers, J.N., McCarthy, J.J., 1969. Half-saturation constants for uptake of nitrate and

- ammonium by marine phytoplankton. *Limn. Oceanogr.* 14, 912-920.
- Estrada, M., Blasco, D., 1985. Phytoplankton assemblages in coastal upwelling areas, in: Bas Peired., C., Margalef, R., Rubiés, P. (Eds.), *Simposio internacional sobre las areas de afloramiento mas importantes del Oeste Africano*, Vol 1. Instituto de Investigaciones Pesqueras, Barcelona, Spain, pp. 397-402.
- FAO, 2016. *The state of world fisheries and aquaculture 2016 – contributing to food security and nutrition for all*. Food and Agriculture Organization of the United Nations.
- Fawcett, S.E., Ward, B.B., 2011. Phytoplankton succession and nitrogen utilization during the development of an upwelling bloom. *Mar. Ecol. Prog. Ser.* 428, 13-21.
- Ferreira, J.G., Andersen, J.H., Borja, A., Bricker, S.B., Camp, J., Cardoso da Silva, M., Garcés, E., Heiskanen, A.S., Humborg, C., Ignatiades, L., Lancelot, C., Menesguen, A., Tett, P., Hoepffner, N., Claussen, U., 2011. Overview of eutrophication indicators to assess environmental status within the European Marine Strategy Framework Directive. *Estuar. Coast Shelf S.* 93:117-131.
- Fleming-Lehtinen, V., Andersen, J.H., Castensen, J., Lysiak-Pastuszek, E., Murray, C., Pyhälä, M., Laamanen, M., 2015. Recent developments in assessment methodology reveal that the Baltic Sea eutrophication problem is expanding. *Ecol. Indic.*, 28, 380-388.
- Furnas, M.J., 1990. In situ growth rates of marine phytoplankton: approaches to measurement, community and species growth rates. *J. Plankton Res.* 12, 1117-1151.
- Gaedeke, A., Sommer, U., 1986. The influence of the frequency of periodic disturbances on the maintenance of phytoplankton diversity. *Oecologia.* 71, 25-28.
- Gibb, S.W., Cummings, D.G., Irigoien, X., Barlow, R.G., Fauzi, R., Mantoura, C., 2001. Phytoplankton pigment chemotaxonomy of the northeastern Atlantic. *Deep-Sea Res. Pt. II*, 48, 795-823.
- Glenn, S., Arnone, R., Bergmann, T., Bissett, W.P., Crowley, M., Cullen, J., Gryzmski, J., Haidvogel, D., Kohut, J., Moline, M., Oliver, M., Orrico, C., Sherrell, R., Song, T., Weidemann, A., Chant, R., Schofield, O., 2004. Biogeochemical impact of summertime coastal upwelling on the New Jersey Shelf. *J. Geophys. Res.*, 109, 1-15.
- Gobler, C.J., Buck, N.J., Sieracki, M.E., Sañudo-Wilhelmy, A., 2006. Nitrogen and silicon limitation of phytoplankton communities in an urban estuary: The East River-Long Island Sound system. *Estuar. Coast. Shelf S.* 68, 127-138.
- Glibert, 2016. Margalef revisited: a new phytoplankton mandala incorporating twelve dimensions, including nutritional physiology. *Harmful Algae*, 55, 25-30.
- Glibert, P.M., Wilkerson, F.P., Dugdale, R.C., Raven, J.A., Dupont, C.L., Leavitt, P.R., Parker, A.E., Burkholder, J.M., Kana, T.M., 2015. Pluses and minuses of ammonium and nitrate uptake and assimilation by phytoplankton and implications for productivity and community composition, with emphasis on nitrogen-enriched conditions. *Limnol. Oceanogr.*, 61, 165-197.
- Goela, P.C., Danchenko, S., Icely, J.D., Lubian, L.M., Cristina, S., Newton, A., 2014. Using

- CHEMTAX to evaluate seasonal and interannual dynamics of the phytoplankton community off the South-west coast of Portugal. *Estuar. Coast. Shelf. S.* 151, 112-123.
- González, H.E., Bernal, P., Ahumada, R., 1987. Desarrollo de dominancia local en la taxocenosis de fitoplâncton de Bahía de Concepción, Chile, durante un evento de surgencia. *Rev. Chilena Hist. Nat.* 60, 19-35.
- González, H.E., Menschel, E., Aparicio, C., Barría, C., 2007. Spatial and temporal variability of microplankton and detritus, and their export to the shelf sediments in the upwelling area off Concepción, Chile (~36°S), during 2002-2005. *Prog. Oceanogr.* 75, 435-451.
- González, H.E., Pantoja, S., Iriarte, J., Bernal, P.A., 1989. Winter-spring variability of size fractionated autotrophic biomass in Concepción Bay, Chile. *J. Plankton Res.* 11:1157–1167.
- Guerrero, M.G., Vega, J.M., Losada, M., 1981. The assimilatory nitrate-reducing system and its regulation. *Ann. Rev. Plant Physiol.* 32, 169-204.
- Hardin, G., 1960. The competitive exclusion principle. *Science* 131, 1292-1297.
- Hasle, G.R., Syvertsen, E.E., 1997. Marine diatoms, in: Tomas, C.R., *Identifying Marine Phytoplankton*. Academic Press, Inc., San Diego, pp. 5-385.
- Helleren, S., 2016. The diatom *Chaetoceros* spp. as a potential contributing factor to fish mortality events in Cockburn Sound, November 2015. Dalcon Environmental Report DE00000.R1.
- Hoppenrath, M., Elbrachter, M., Drebes, G., 2009. *Marine Phytoplankton. Selected Microphytoplankton Species from the North Sea Around Helgoland and Sylt*. E. Schweizerbart'sche Verlagsbuchhandlung, Stuttgart, Germany.
- Hormazabal, S., Shaffer, G., Letelier, J., Ulloa, O., 2001. Local and remote forcing of the sea surface temperature in the coastal upwelling system off Chile. *J. Geophys. Res.*, 16:16657-16671.
- Huszar, V.L. de M., Caraco, N.F., 1998. The relationship between phytoplankton composition and physical-chemical variables: a comparison of taxonomic and morphological-functional descriptors in six temperate lakes. *Freshwater Biol.* 40, 679-696.
- Hutchins, D.A., DiTullio, G.R., Zhang, Y., Bruland, K.W., 1998. An iron limitation mosaic in the California upwelling regime. *Limnol. Oceanogr.* 43, 1037-1054.
- Hutchins, D.A., Hare, C.E., Weaver, R.S., Zhang, Y., Firme, G.F., DiTullio, G.R., Alm, M.B., Riseman, S.F., Maucher, J.M., Geesey, M.E., Trick, C.G., Smith, G.J., Rue, E.L., Conn, J., Bruland, K.W., 2002. Phytoplankton iron limitation in the Humboldt Current and Peru Upwelling. *Limnol. Oceanogr.* 47, 997-1011.
- Irigoién, X., Meyer, B., Harris, R., Harbour, D., 2004. Using HPLC pigment analysis to investigate phytoplankton taxonomy: the importance of knowing your species. *Helgol. Mar. Res.* 58, 77-82.
- Ji, Y., Sherrell, R.M., 2008. Differential effects of phosphorus limitation on cellular metals in *Chlorella* and *Microcystis*. *Limnol. Oceanogr.* 53, 1790–1804.

- Jeffrey, S.W., 1974. Profiles of photosynthetic pigments in the ocean using thin-layer chromatography. *Mar. Biol.* 26, 101-110.
- Koch, P., Rivera, P., 1984. Contribución al conocimiento de las diatomeas chilenas III: el género *Chaetoceros* Ehr. (subgénero *Phaeoceros* Gran). *Gayana. Bot.*, 41, 61-84.
- Lampert, L., Perrot, L., Delmas, D., 2016. Analyse chénotaxonomique de la campagne TIC-MOC (mars 2015): Projet CALHIS. IFREMER – Département Océanographie et Dynamique des Écosystèmes.
- Lassiter, A.M., Wilkerson, F.P., Dugdale, R.C., Hogue, V.E., 2006. Phytoplankton assemblages in the CoOP-WEST coastal upwelling area. *Deep-Sea Res. Pt. II*, 3063-3077
- Laza-Martinez, A., Seoane, S., Zapata, M., Orive, E., 2007. Phytoplankton pigment patterns in a temperate estuary: from unialgal cultures to natural assemblages. *J. Plankton Res.* 11, 913-929.
- Lomas, M.W., Glibert, P.M., 1999a. Temperature regulation of nitrate uptake: a novel hypothesis about nitrate uptake and reduction in cool-water diatoms. *Limnol. Oceanogr.* 44, 556-572.
- Lomas, M.W., Glibert, P.M., 1999b. Interactions between NH_4^+ and NO_3^- uptake and assimilation: comparison of diatoms and dinoflagellates at several growth temperatures. *Mar. Biol.* 133, 541-551.
- Lomas, M.W., Glibert, P.M., 2000. Comparisons of nitrate uptake, storage and reduction in marine diatoms and flagellates. *J. Phycol.* 36, 903-913.
- Lund, J.W.G., Kipling, C., Le Cren, E.D., 1958. The invert microscope method of estimating algal numbers and the statistical basis of estimations by counting. *Hydrobiologia* 11, 143-170.
- Mackey, M., Mackey, D., Higgins, H., Wright, S., 1996. CHEMTAX e a program for estimating class abundances from chemical markers: application to HPLC measurements of phytoplankton. *Mar. Ecol. Prog. Ser.* 144, 265-283.
- Margalef, R., 1978. Life-forms of phytoplankton as survival alternatives in an unstable environment. *Oceanol. Acta*, 1, 493-509.
- Margalef, R., Estrada, M., Blasco, D. 1979. Functional morphology of organisms involved in red tides, as adapted to decaying turbulence, in: Taylor, D.L., Seliger, H.H. (Eds.), *Toxic Dinoflagellate Blooms*. Elsevier-North Holland, Amsterdam, pp. 89-94.
- McKay, R.M.L., Villareal, T.A., La Roche, J., 2000. Vertical migration by *Rhizosolenia* spp. (Bacillariophyceae): implications for Fe acquisition. *J. Phycol.* 36, 669-674.
- Montecino, V., Astoreca, R., Alarcón, G., Retamal, L., Pizarro, G., 2004. Bio-optical characteristics and primary productivity during upwelling and non-upwelling conditions in a highly productive coastal ecosystem off Central Chile (~36°S). *Deep-Sea Res. Pt. II*. 51:2413–2426.
- Nixon, S.W., 1995. Coastal marine eutrophication: a definition, social causes, and future concerns. *Ophelia*. 41:199-219.

- OSPAR Commission, 2010. The North-East Atlantic environment strategy: strategy of the OSPAR Commission for the protection of the marine environment of the North-East Atlantic 2010-2020. OSPAR Agreement 2010-3.
- Owens, O.V.H. and Esaias, W., 1976. Physiological responses of phytoplankton to major environmental factors. *Annu. Rev. Plant Phys.* 27:461-483.
- Padisák, J., Reynolds, C.S., 1998. Selection of phytoplankton associations in Lake Balaton, Hungary, in response to eutrophication and restoration measures, with special reference to the cyanoprokaryotes. *Hydrobiologia*, 384, 41-53.
- Parsons, T.R., Harrison, P.J., Waters, R., 1978. An experimental simulation of changes in diatom and flagellate blooms. *J. Exp. Mar. Biol. Ecol.* 32, 285-294.
- Peterson, W.T., Arcos, D.F., McManus, G.B., Dam, H., Bellantoni, D., Johnson, T., Tiselius, P., 1988. The nearshore zone during coastal upwelling: daily variability and coupling between primary and secondary production off Central Chile. *Prog. Oceanogr.* 20:1-40.
- Pitcher, G.C., 1990. Phytoplankton seed populations of the Cape Peninsula upwelling pule, with particular reference to resting spores of *Chaetoceros* (Bacillariophyceae) and their role in seeding upwelling waters. *Estuar. Coast. Shelf. S.* 31, 283-301.
- Post, A.F., Dubinsky, Z., Wyman, K., Falkowski, P.G., 1984. Kinetics of light-intensity adaptation in a marine planktonic diatom. *Mar. Biol.* 83, 231-238.
- Prézelin, B.B., Matlick, H.A., 1983. Nutrient-dependent low-light adaptation in the dinoflagellate *Gonyaulax polyedra*. *Mar. Biol.* 74, 141-150.
- Prézelin, B.B., Tilzer, M.M., Schofield, O., Haese, C., 1991. The control of the production process of phytoplankton by the physical structure of the aquatic environment with special reference to its optical properties. *Aquat. Sci.*, 53, 136-186.
- Redfield, A.C., 1934. On the proportions of organic derivatives in sea water and their relation to the composition of plankton, in: Daniel, R.J. (Ed.) *The James Johnstone Memorial Volume*. Liverpool University Press, Liverpool.
- Redfield, A.C., 1958. The biological control of chemical factors in the environment. *Am. Sci.* 46:205-221.
- Reynolds, C.S., 1984. *The ecology of freshwater phytoplankton*. Cambridge University Press, Cambridge.
- Reynolds, C.S., 1987. Community organization in the freshwater plankton. *Symp. Br. Ecol. Soc.*, 27:297-325.
- Reynolds, C.S., 1988. Functional morphology and the adaptive strategies of freshwater phytoplankton, in: Sandgren, C.D. (Ed.), *Growth and reproductive strategies of freshwater phytoplankton*. Cambridge University Press, Cambridge, pp. 388-433.
- Reynolds, C.S., 1996. Plant life of the pelagic. *Proc. Int. Assoc. Theor. Appl. Limnol.* 26, 97-113.

- Reynolds, C.S., 2006. The ecology of phytoplankton. Cambridge University Press, Cambridge.
- Ricard, M., 1987. Atlas du Phytoplancton Marin. II. Diatomophycees. Centre National de la Recherche Scientifique, Paris, France.
- Rivkin, R.B., Voytek, M.A., Seliger, H.H., 1982. Phytoplankton division rates in light-limited environments: two adaptations. *Science* 215, 1123-1125.
- Rodhe, W., 1969. Crystallization of eutrophication concepts in northern Europe, in: Eutrophication: causes, consequences, correctives. National Academy of Sciences, Washington, DC, pp. 50-64.
- Romero, O.E., Hebbeln, D., 2001. Temporal and spatial variability in export production in the SE Pacific Ocean: evidence from siliceous plankton fluxes and surface sediment assemblages. *Deep-Sea Res.* 48, 2673-2697.
- Romero, O.E., Hebbeln, D., 2003. Biogenic silica and diatom thanatocoenosis in surface sediments below the Peru-Chile Current: controlling mechanisms and relationship with productivity of surface waters. *Mar. Micropaleontol.* 43, 71-90.
- Roy, S., 1989. HPLC-measured chlorophyll-type pigments during a phytoplankton spring bloom in Bedford Basin (Canada). *Mar. Ecol. Prog. Ser.* 33, 279-290.
- Roy, S., Llewellyn, C., Egelend, E.S., Johnsen, G., 2011. Phytoplankton pigments: characterization and applications in oceanography. Cambridge University Press, Cambridge.
- Sanders, J.G., Cibik, S.J., D'Elia, C.F., Boynton, W.R., 1987. Nutrient enrichment studies in a coastal plain estuary: changes in phytoplankton species composition. *Can. J. Fish. Aquat. Sci.* 44, 83-90.
- Sarmiento, J.L., Gruber, N., 2006. Ocean biogeochemical dynamics. Princeton University Press, New Jersey.
- Sarthou, G., Timmermans, K.R., Blain, S., Tréguer, P., 2005. Growth physiology and fate of diatoms in the ocean: a review. *J. Sea Res.* 53, 25-42.
- Schindler, D.W., 1987. Detecting ecosystem responses to anthropogenic stress. *Can. J. Fish. Aquat. Sci.* 44, 6-25.
- Schlüter, L., Møhlenberg, F., Havskum, H., Larsen, S., 2000. The use of phytoplankton pigments for identifying and quantifying phytoplankton groups in coastal areas: testing the influence of light and nutrients on pigment/chlorophyll *a* ratios. *Mar. Ecol. Prog. Ser.* 192, 49-63.
- Schuman, F.R., Lorenzen, C.J., 1974. Quantitative degradation of chlorophyll by a marine herbivore. *Limnol. Oceanogr.* 20, 580-586.
- Seoane, S., Zapata, M., Orive, E., 2009. Growth rates and pigment patterns of haptophytes isolated from estuarine waters. *J. Sea Res.* 62, 286-294.
- Smayda, T.J., Reynolds, C.S., 2001. Community assembly in marine phytoplankton: application of recent models to harmful dinoflagellate blooms. *J. Plankton Res.* 23, 447-461.
- Smayda, T.J., Reynolds, C.S., 2003. Strategies of marine dinoflagellate survival and some rules of

- assembly. *J. Sea Res.* 49, 95-106.
- Smith, V.H., Tilman, G.D., Nekola, J.C., 1999. Eutrophication: impacts of excess nutrient inputs on freshwater, marine, and terrestrial ecosystems. *Environ. Pollut.* 100, 179-196.
- Sournia, A., 1986. Atlas du Phytoplancton Marin. I. Introduction, Cyanophycées, Dictyophycées, Dinophycées et Raphidophycées. Centre National de la Recherche Scientifique, Paris, France.
- Stambler, N., Dubinsky, Z., 2007. Marine phototrophs in the twilight zone, in: Seckbach, J. (Ed.), *Algae and cyanobacteria in extreme environments*. Springer, Dordrecht, pp. 79-97.
- Stockner, J.G., Shortreed, K.R.S., 1978. Enhancement of autotrophic production by nutrient addition in a coastal rainforest stream on Vancouver Island. *J. Fish. Res. Board. Can.* 35, 28-34.
- Sundbäck, K., Snoeijs, P., 1991. Effects of nutrient enrichment on microalgal community composition in a coastal shallow-water sediment system: an experimental study. *Bot. Mar.*, 34, 341-358.
- Sukenik, A., Bennet, J., Mortain-Bertrand, A., Falkowski, P.G., 1990. Adaptation of the photosynthetic apparatus to irradiance in *Dunaliella tertiolecta*. *Plant. Physiol.* 92, 891-898.
- Thiel, M., Macaya, E.C., Acuña, E., Arntz, W.E., Bastias, H., Brokordt, K., Camus, P.A., Castilla, J.C., Castro, L.R., Cortés, M., Dumont, C.P., Escribano, R., Fernandez, M., Gajardo, J.A., Gaymer, C.F., Gomez, I., González, A.E., González, H.E., Haye, P.A., Illanes, J., Iriarte, J.L., Lancellotti, D.A., Luna-Jorquera, G., Luxoro, C., Manriquez, P.H., Marín, V., Muñoz, P., Navarrete, S.A., Perez, E., Poulin, E., Sellanes, J., Sepúlveda, H.H., Stotz, W., Tala, F., Thomas, A., Vargas, C.A., Vasquez, J.A., Veja, A.J.M., 2007. The Humboldt current system of Northern and Central Chile: oceanographic processes, ecological interactions and socioeconomic feedback. *Oceanogr. Mar. Biol.* 45, 195-344.
- Thomas, W.H., Seibert, D.L.R., Dodson, A.N., 1974. Phytoplankton enrichment experiments and bioassays in natural coastal sea water and in sewage outfall receiving waters off southern California. *Estuar. Coast. Mar. Sci.* 2, 191-206.
- Tilman, D., Kilham, S.S., Kilham, P., 1982. Phytoplankton community ecology: the role of limiting nutrients. *Annu. Rev. Ecol. Syst.* 13, 349-372.
- Tomas, C., 1997. *Identifying Marine Phytoplankton*. Academic Press, San Diego.
- Torres, R., Ampuero, P., 2009. Strong CO₂ outgassing from high nutrient low chlorophyll coastal waters off central Chile (30°S): the role of dissolved iron. *Estuar. Coast. Shelf. S.* 83, 126-132.
- Utermohl, H., 1958. Zur Vervollkommnung der quantitativen Phytoplankton- Methodik. *Mitt. Int. Ver. Limnol.* 9, 1-38.
- Van Oostende, N., Dunne, J.P., Fawcett, S.E., Ward, B.B., 2015. Phytoplankton succession explains size-partitioning of new production following upwelling-induced blooms. *J. Marine. Syst.* 148, 14-25.
- Vernet, M., Lorenzen, C.J., 1987. The relative abundance of pheophorbide *a* and pheophytin *a* in temperate marine waters. *Limnol. Oceanogr.* 32, 352-358.

- Wang, D., Gouhier, T.C., Menge, B.A., Ganguly, A.R. 2015. Intensification and spatial homogenization of coastal upwelling under climate change. *Nature* 518, 390-394.
- Williams, P.J.B., Thomas, D.N., Reynolds, C.S., 2002. *Phytoplankton productivity: carbon assimilation in marine and freshwater ecosystems*. Blackwell Science, Oxford.
- Wright, S.W., Thomas, D.P., Marchant, J., Higgins, H.W., Mackey, M.D., Mackey, D.J., 1996. Analysis of phytoplankton of the Australian sector of the Southern Ocean: comparisons of microscopy and size frequency data with interpretations of pigment HPLC data using the 'CHEMTAX' matrix factorisation program. *Mar. Ecol. Prog. Ser.* 144, 285-298.
- Wright, S.W., Ishikawa, A., Marchant, H.J., Davidson, A.T., van den Enden, R.L, Nash, G.V., 2009. Composition and significance of picophytoplankton in Antarctic waters. *Polar Biol.* 32, 797-808.
- Yang, C.Z., Albright, L.J., 1992. Effects of the harmful diatom *Chaetoceros concavicornis* on respiration of rainbow trout *Oncorhynchus mykiss*. *Dis. Aquat. Org.* 14, 105-114.
- Yentsch, C.S., 1967. The measurement of chloroplastic pigments - thirty years of progress?, in: Golterman, H.L., Clymo, R.S. (Eds.), *Chemical environment in the aquatic habitat: proceedings of an I.B.P.-symposium held in Amsterdam and Nieuwersluis on 10-16 October 1966*. North-Holland, Amsterdam, pp.255-270.
- Zapata, M., Rodríguez, F., Garrido, J.L., 2000. Separation of chlorophylls and carotenoids from marine phytoplankton: a new HPLC method using a reversed phase C₈ column and pyridine-containing mobile